Geobiology 2013 Lecture 5

Biogeochemical Tracers

Isotopics #2: C, H, O and N

Acknowledgements: John Hayes, Karen Casciotti, Steve Macko, John Hedges

Assigned Reading

- Stanley 2nd Ed Chapter 10, pp 221-240

- Hayes JM 2001 Fractionation of the isotopes of carbon and hydrogen in biosynthetic processes. Reviews in Mineralogy *Stable Isotopic Geochemistry*, John W. Valley and David R. Cole (eds.)
- Hayes Concepts and Calculations

Geobiology 2012 Lecture 5

Biogeochemical Tracers

Isotopics #2: C, H, O and N

Need to Know:

Ballpark delta values of C, O, N, H in marine and terrestrial biomass

How H&O are fractionated in the hydrological cycle

How (roughly) C&H fractionation occurs in organic matter

How (roughly) N is fractionated on land and in the ocean

Sources of hydrogen and oxygen isotopic fractionation

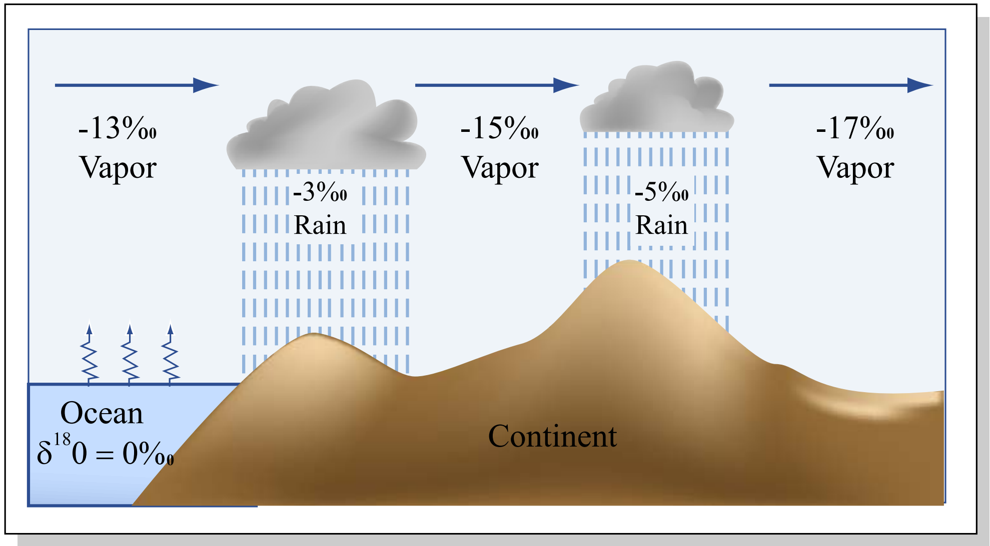

Figure by MIT OpenCourseWare.

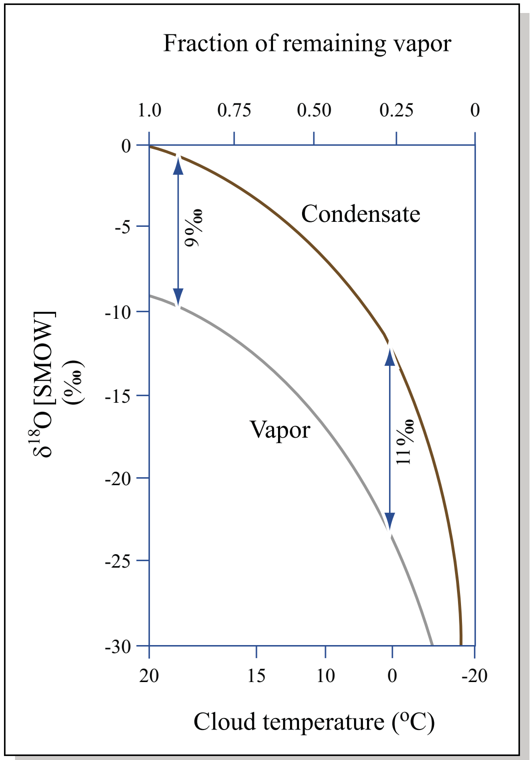

Figure by MIT OpenCourseWare.

Image removed due to copyright restrictions.
Graph of deuterium per mil over oxygen-18 per mil.

The major nonbiological fractionation process affecting stable hydrogen (and oxygen) isotopes is the hydrologic cycle in which water molecules containing lighter isotopes (^{1}H & ^{16}O) are preferentially evaporated and retained in a cloud (vs. ^{2}H & ^{18}O).

The net result of this fractionation process is that precipitation at increasingly inland, higher altitude (cooler) sites is depleted in both ^{18}O and ^{2}H (D).

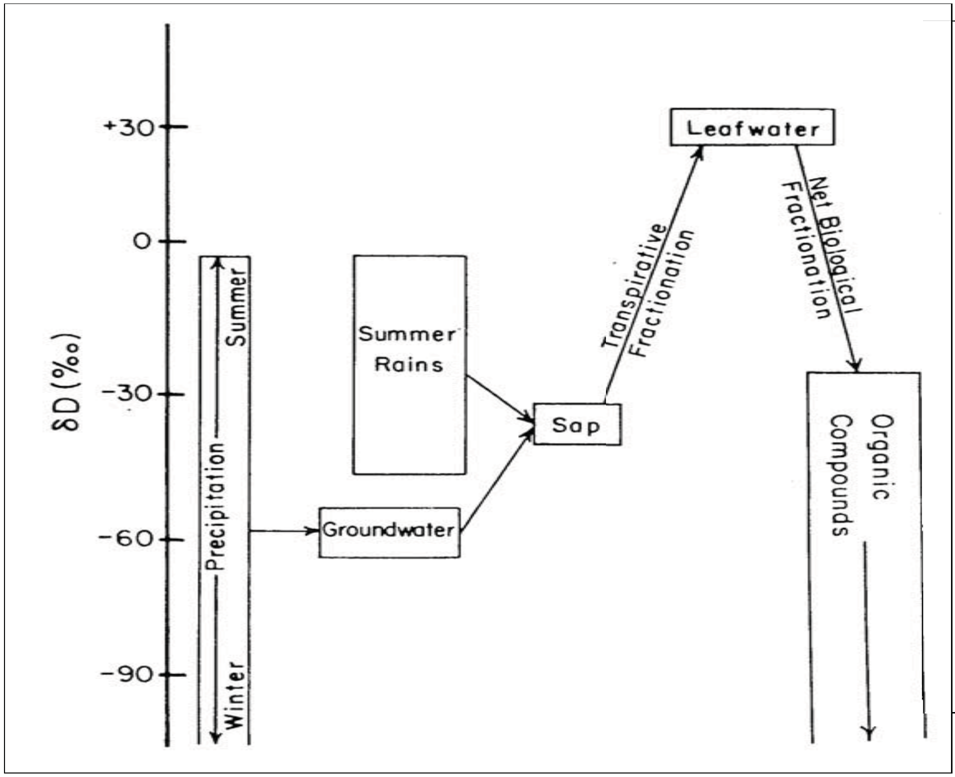

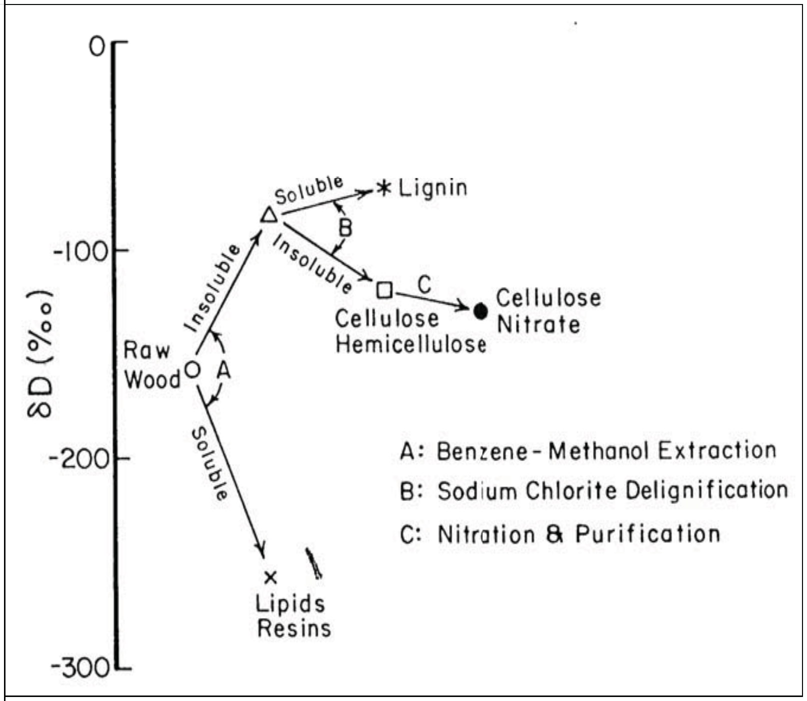

Courtesy of John Hayes. Used with permission.

In general, tree sap isotopically resembles local meteoric water, whereas leaf water is isotopically enriched. Organic matter is depleted in D versus the leaf water from which it is biosynthesized (values given above are typical for N. American plants).

In general, lipids are depleted in D versus lignin and cellulose from the same plant, whereas cellulose is slightly more depleted than coexisting lignin (Rundle et al., 1989).

Cellulose is usually analyzed in nitrated form (NO_3 replacing OH on each C), so that only the nonexchangeable H directly bound to C is analyzed.

Because the D in cellulose nitrate reflects local water, woods can be used as a proxy for the hydrogen isotope composition of past environments in which the wood was made

Hydrogen isotopic signatures

Photosynthesis $H_2O + hv \rightarrow O_2 + NADPH$ *Fd-NADP reductase* (2.4)

2 reduced ferredoxin + $NADP^+ + H^+$ 2 oxidized ferredoxin + NADPH

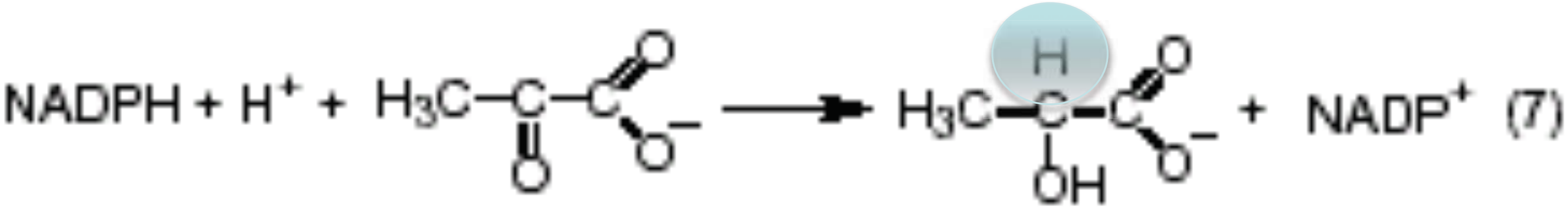

Insertion of a non-exchangeable H^- from NADPH into pyruvate.

Reactions like this responsible for setting δD of organics

H going from NADPH to pyruvate becomes H in lipid

Hydrogen isotopic signatures inherited from water through reactions of NADPH

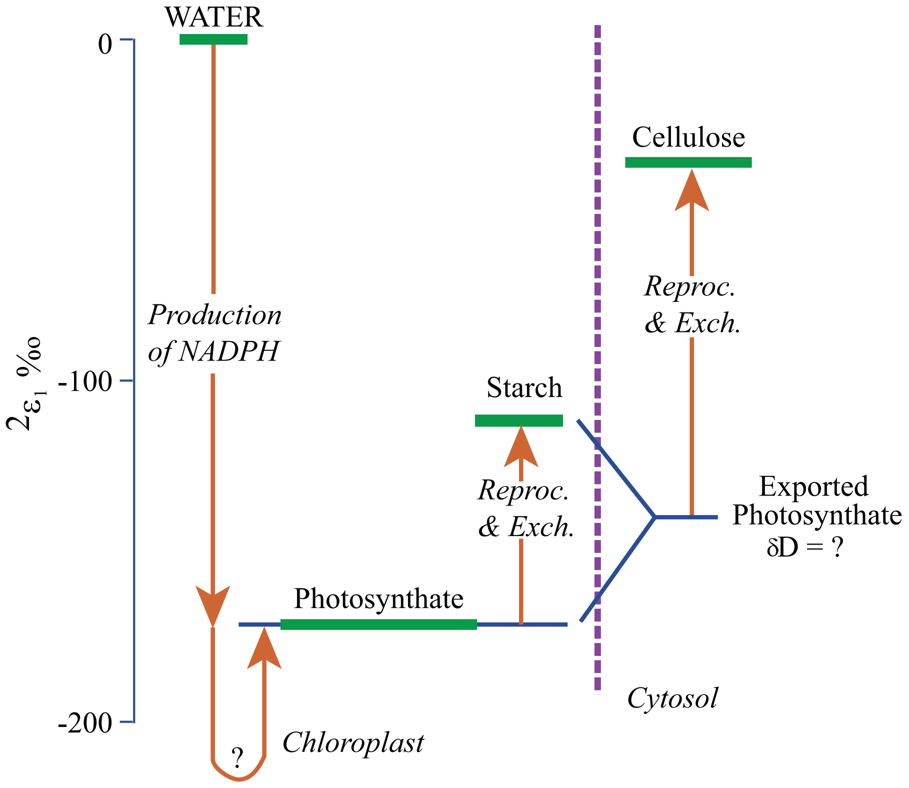

Relationships between the hydrogen isotopic compositions of initial photosynthate and related products and of water available within plant cells. The uncertainty indicated on the pathway between water and photosynthate reflects the possibility of offsetting fractionations in the production of NADPH and the subsequent transfer of H^- to photosynthate.

Figure by MIT OpenCourseWare.

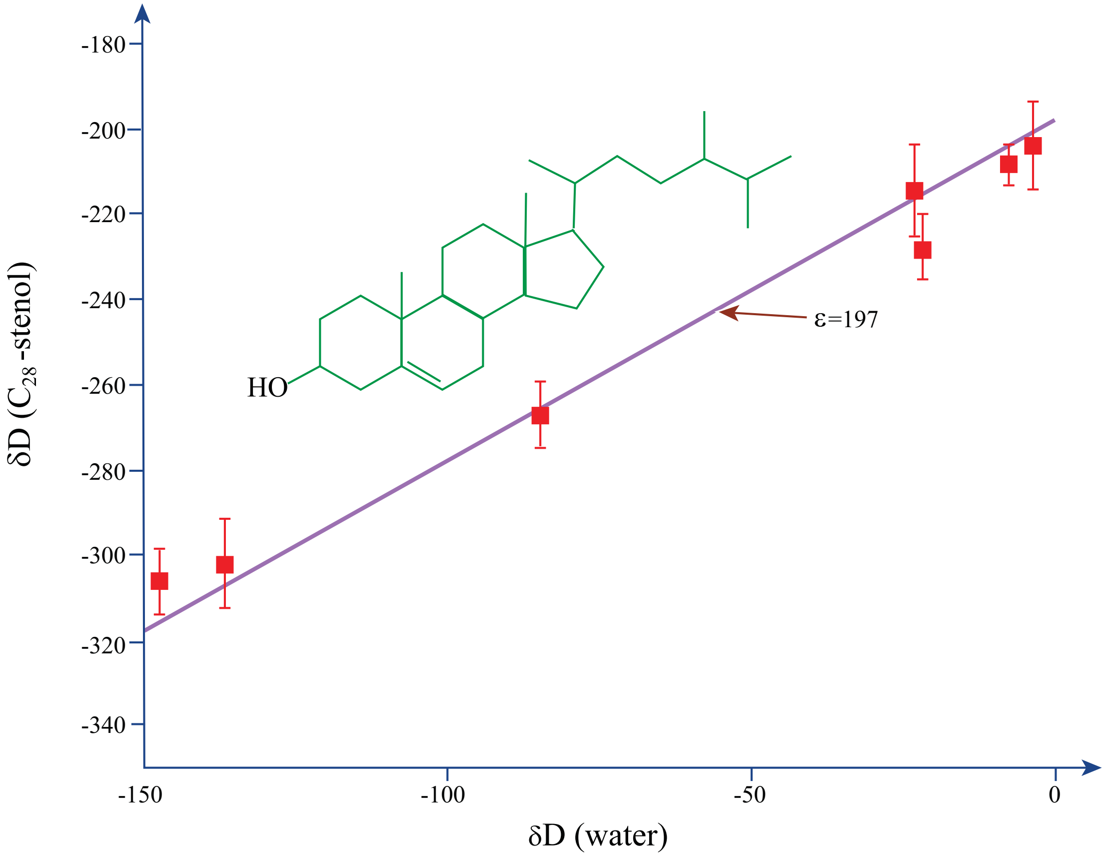

Relationship between D/H ratios (δD, in ‰ Vienna standard mean ocean water (SMOW)) for the C_{28} stenol biosynthesized by phytoplankton grown in different lakes and marine enviroments and that of the ambient waters (modified after *Sauer et al*. [2001]). The line represents constant fractionations ε. It is apparent that the sterol is recording the D/H ratio of the ambient water. Hence the δD value of sedimentary sterols should permit proxy estimation of the δD of past water bodies, a key feature of paleohydrology.

Figure by MIT OpenCourseWare.

Sources of nitrogen isotopic fractionation

Simplified Terrestrial Nitrogen Cycle

Schematic figure of the nitrogen cycle removed due to copyright restrictions.

http://www.windows.ucar.edu/earth/climate/images/nitrogencycle.jpg

Bottom line: In natural systems, new fixed nitrogen entering the system comes from bacterial nitrogen fixation which results in only small N-isotopic fractionations

Some Typical ^{15}N values

Atm. N_2 ‘fixed’’ by terrestrial flora (Nif in legumes) ~ 0 per mil

Atm. N_2 ‘fixed’ by marine bacteria and Cb ~ 0 per mil

Nitrate or ammonium utilized by terrestrial flora and converted to organic nitrogen ~0 per mil

Dissolved nitrate in the ocean ~ +7 to +10 per mil

Marine organisms high in the trophic structure (e.g. fish, whales)

+10 to + 20 per mil

Simplified Marine Nitrogen Cycle

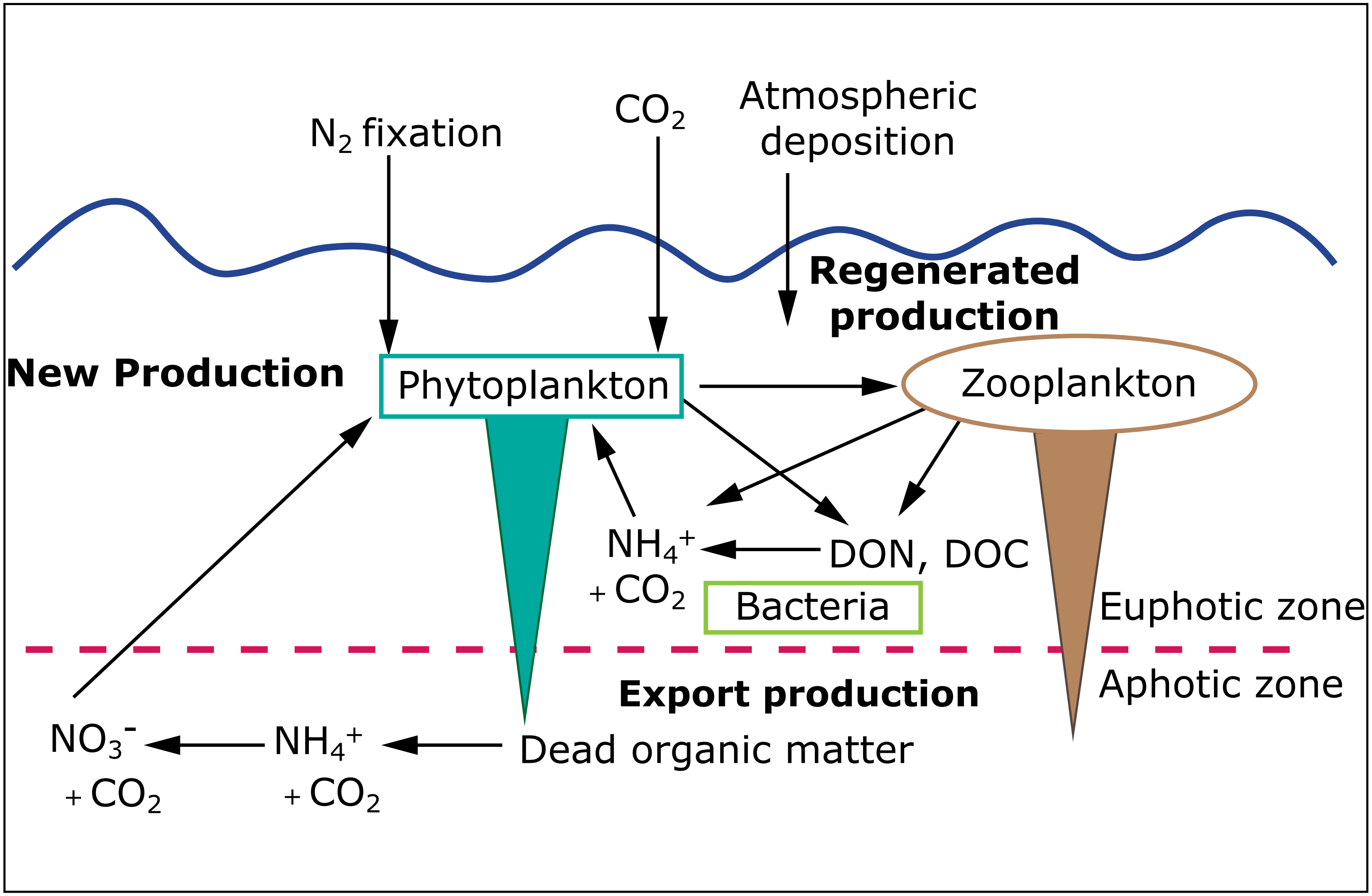

Image by MIT OpenCourseWare.

© Karen Casciotti OCW

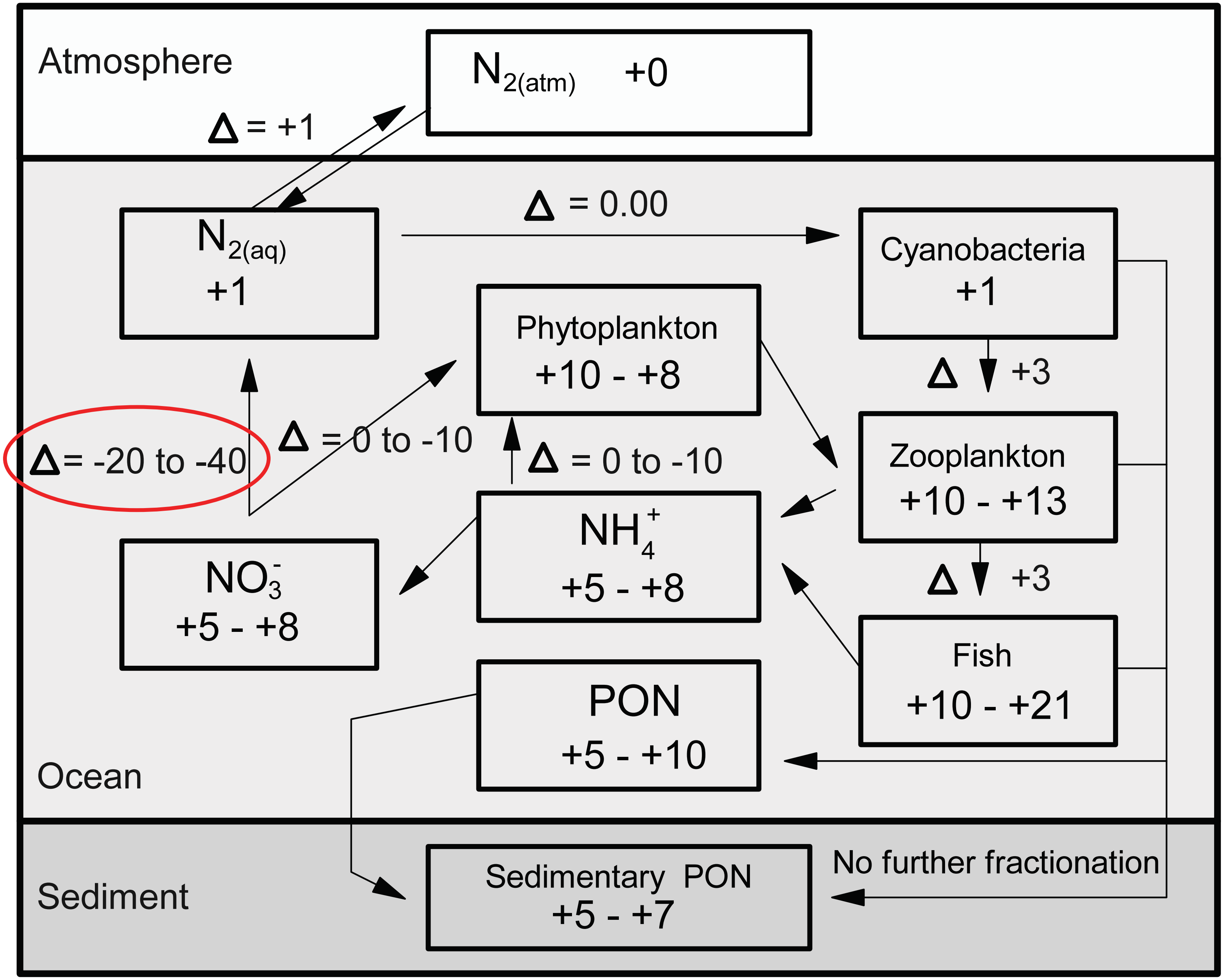
Atmosphere
$N_{2(atm)}$ +0
Δ = +1
$N_{2(aq)}$ +1
Δ = 0.00
Cyanobacteria +1
Phytoplankton +10 - +8
Δ +3
Zooplankton +10 - +13
Δ = -20 to -40
Δ = 0 to -10
Δ = 0 to -10
NH_4^+ +5 - +8
NO_3^- +5 - +8
Δ +3
Fish +10 - +21
PON +5 - +10
Ocean
Sediment
Sedimentary PON +5 - +7
No further fractionation

U. Weismann, “Biological nitrogen removal from wastewater”, Adv. Biochem.Engr. 51:113-154 (1994)

Nitrification:

$$NH_4^+ + 1.5\ O_2 \dashrightarrow NO_2^- + H_2O + 2H^+$$

lowers pH

$$NO_2^- + 0.5\ O_2 \dashrightarrow NO_3^-$$

Denitrification:

$$5\ HOAc + 8\ NO_3^- \dashrightarrow \overset{\text{escapes}}{\boxed{4\ N_2}} + 10\ CO_2 + 6\ H_2O + 8\ OH^-$$

MUST have carbon source, e.g., acetate raises pH

Image by MIT OpenCourseWare.

Major isotopic fractionation in the N-cycle occurs during denitrification (-20 to -40 per mil)

Light N_2 leaves the ocean causing the residual nitrate to become heavy

15N vs 13C Foodweb

Trophic fractionation of carbon and nitrogen isotopes (Georges Bank)

B. Fry (1988) *Limnol. Oceanogr.* **33**, 1182-1190.

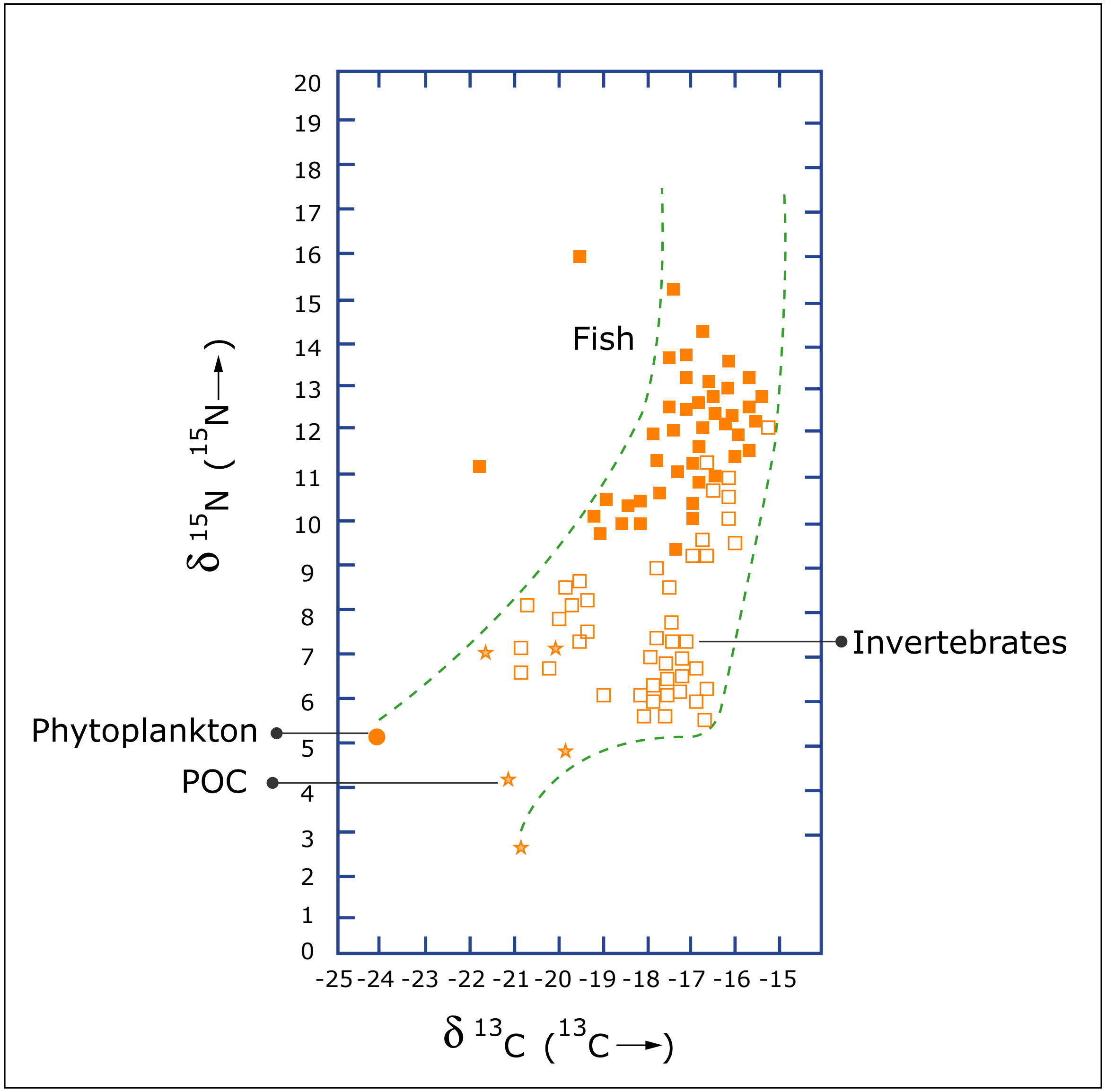

Image by MIT OpenCourseWare.

Trophic fractionation of carbon and nitrogen isotopes

K. Yoshii, N. G. Melnick, O. A. Timoshkin, N. A. Bondarenko, P. N. Anoshko, T. Yoshioka, & E. Wada (1999) *Limnol. Oceanogr.* **44**, 502-511.

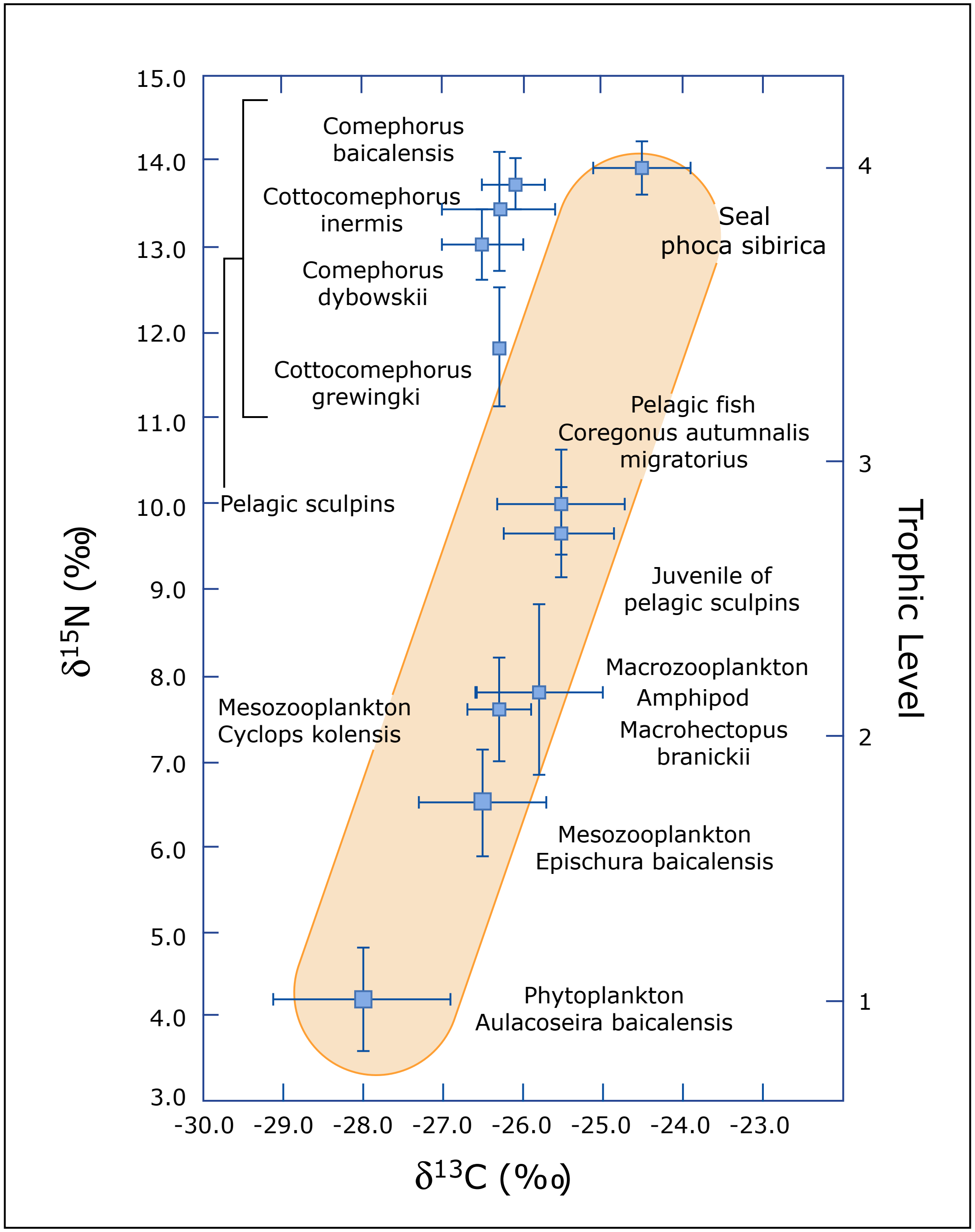

Image by MIT OpenCourseWare.

Biogeochemistry of the Stable Nitrogen Isotopes

An important use of stable nitrogen isotopes is as an indicator of trophic level in natural systems with known nitrogen sources and relatively simple food webs. The following figure is from Schoeninger and DeNiro (1984) GCA 48, 625-639. Average δ15N trophic offset is ~3 ‰ per trophic level

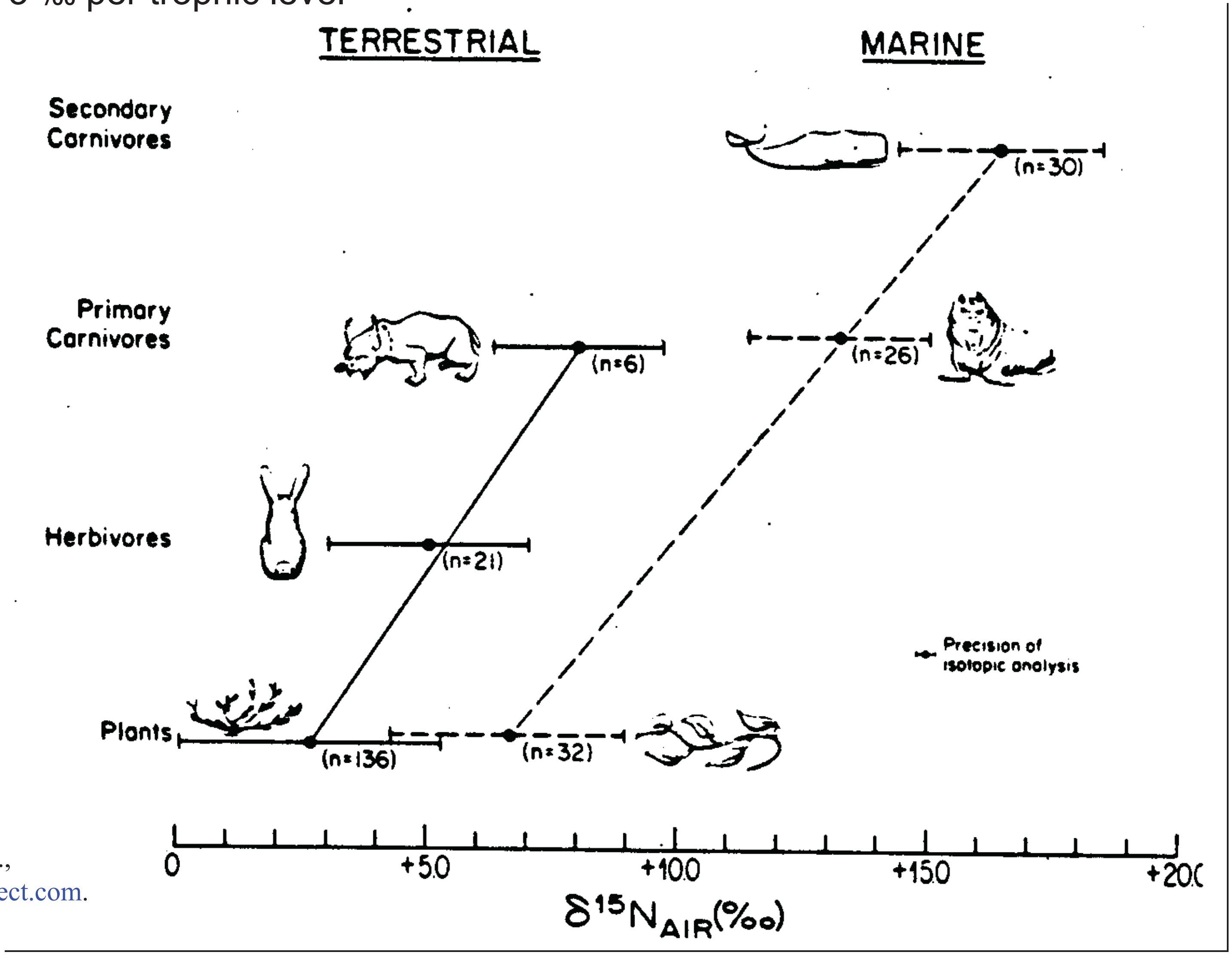

Courtesy Elsevier, Inc., http://www.sciencedirect.com. Used with permission.

Characterizing Organic Matter Using Bulk Isotopic Data

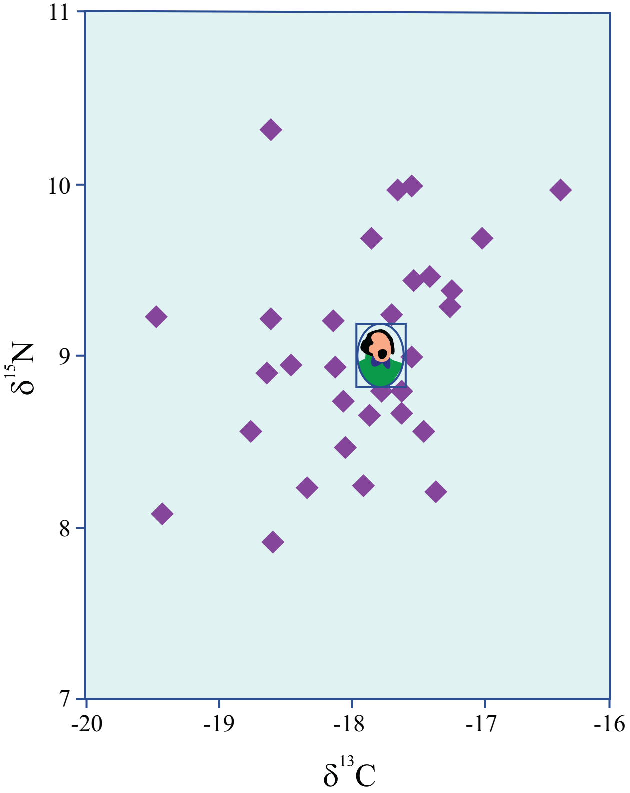

Twin element stable isotope distributions ($\delta^{13}C$ and $\delta^{15}N$, in ‰ versus PDB and air, respectively) of hair samples taken from individual students at the University of Virginia (modified after *Macko et al*. [1998]). Hair is largely composed of the fibrous protein α-keratin. Its isotope composition is reflective of the recent diet of an individual, generally increasing slightly (1‰ in $\delta^{13}C$ and 3‰ in $\delta^{15}N$) with tropic level. The marked variability accords with the great diversity of modern diets. For comparison, George Washington's hair sample testifies to a rather balanced diet.

Figure by MIT OpenCourseWare.

Organismal Variability in Bulk C-Isotopes

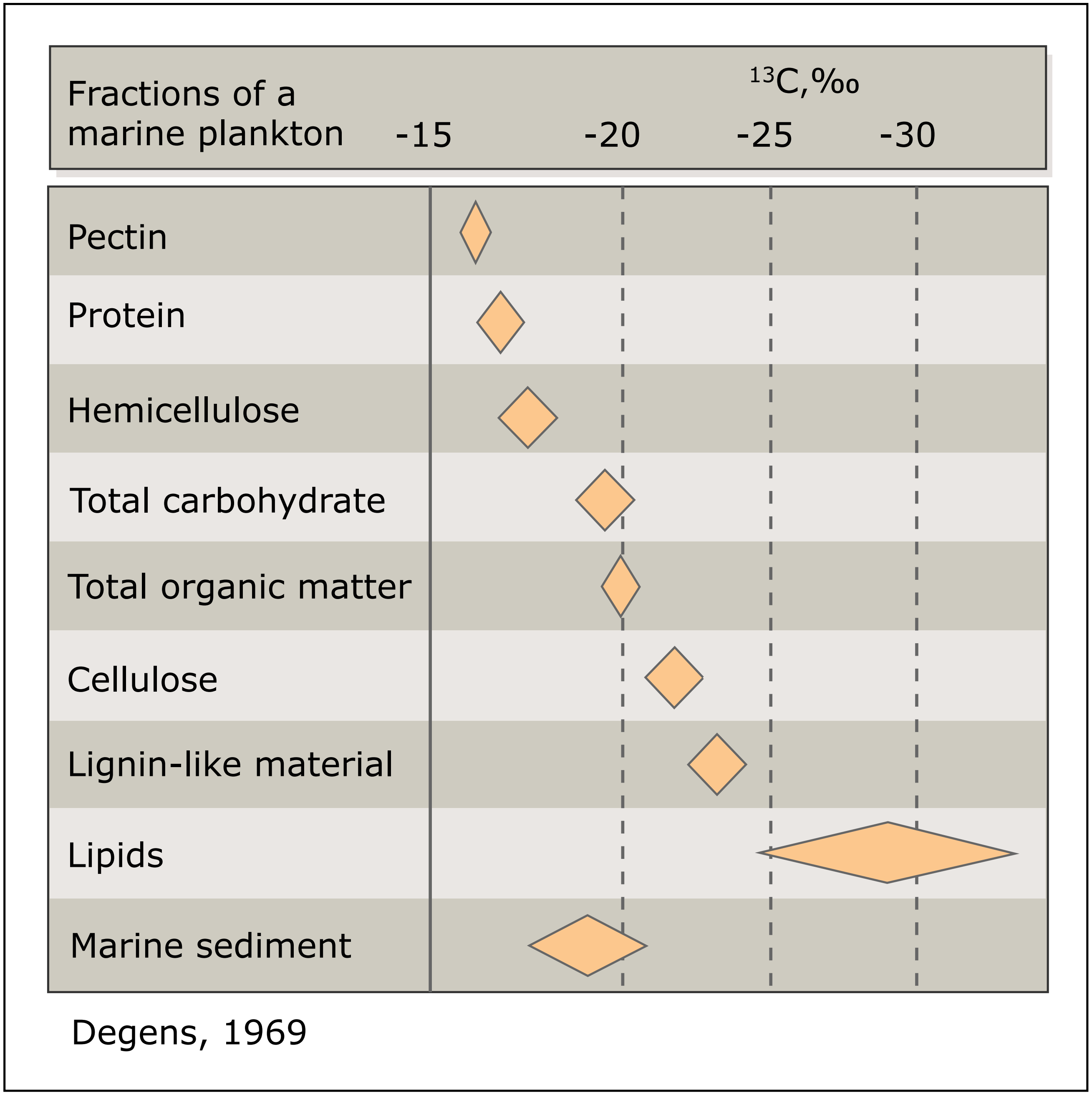

Image by MIT OpenCourseWare.

Multi-element, Compound-specific Isotopic Analyses

Vanillin

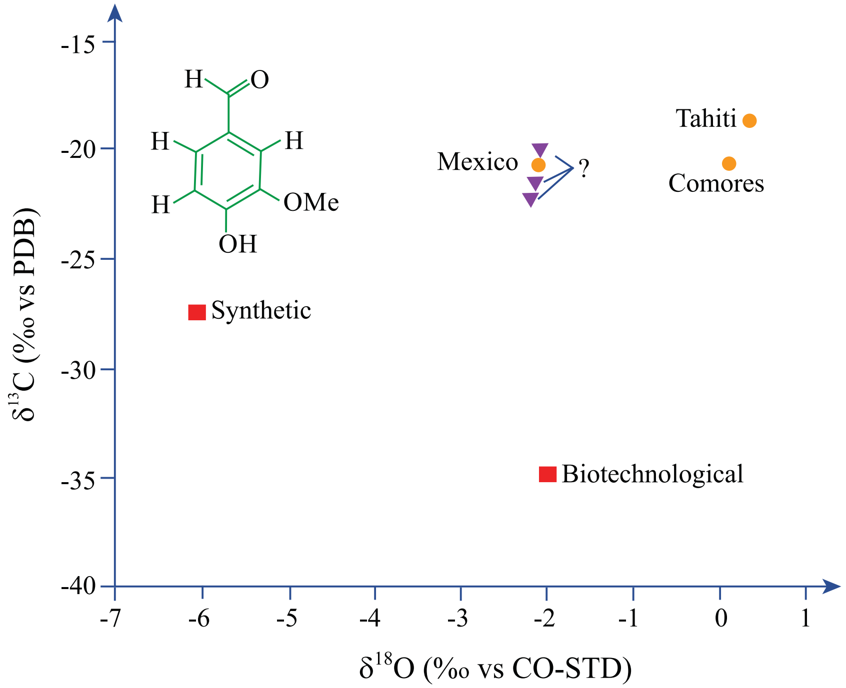

Dual isotopic ($\delta^{13}C$ and $\delta^{18}O$, in ‰ versus PDB and of standard CO, respectively) for the flavor compound vanillin. The three vanillin extracts from the naturally grown vanilla beans have similar $\delta^{13}C$ values, even though they come from geographically widely spaced sites: Mexico and the islands of the Comores and Tahiti. The Mexican sample, however, does differ markedly in $\delta^{18}O$, no doubt owing to major differences in $\delta^{18}O$ in the ambient water supply. Not surprisingly, major differences in both $\delta^{13}C$ and $\delta^{18}O$ are apparent in the synthetic and biotechnological products [*Hener et al., 1998*]. On the basis of their dual isotopic values, the three samples of unknown origin can be assigned to Mexico.

Figure by MIT OpenCourseWare.

Characterising Cocaine Sources

These images have been removed due to copyright restrictions.

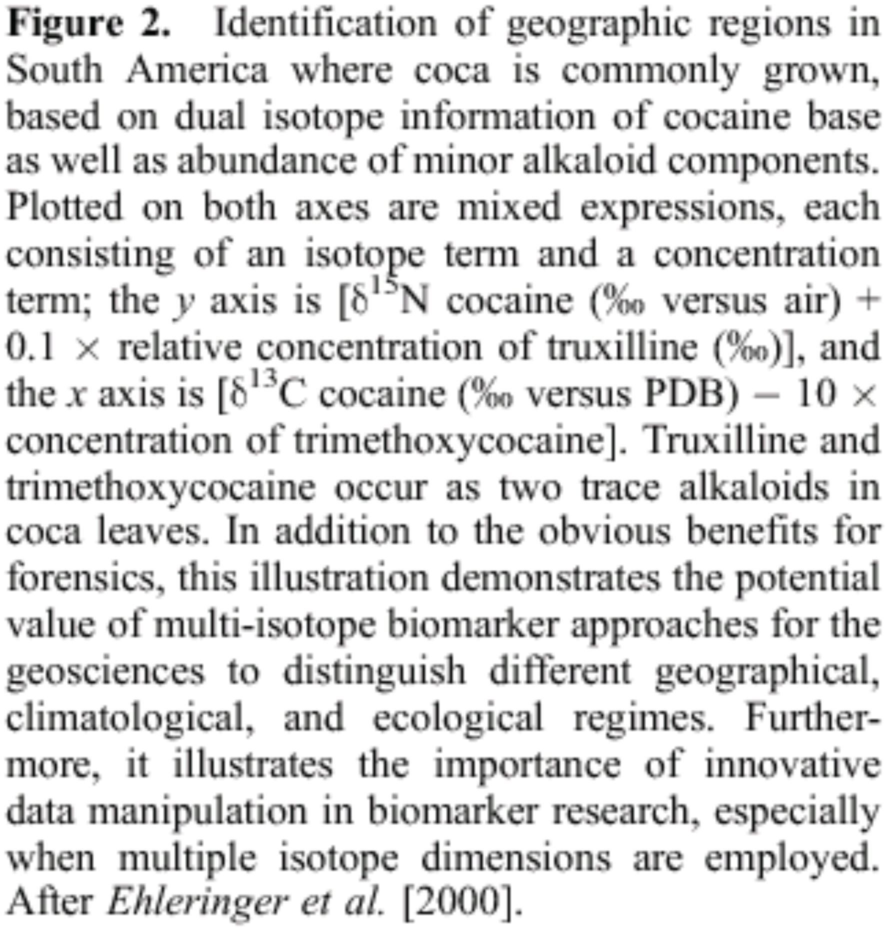

Figure 2. Identification of geographic regions in South America where coca is commonly grown, based on dual isotope information of cocaine base as well as abundance of minor alkaloid components. Plotted on both axes are mixed expressions, each consisting of an isotope term and a concentration term; the *y* axis is [δ^{15}N cocaine (‰ versus air) + 0.1 × relative concentration of truxilline (‰)], and the *x* axis is [δ^{13}C cocaine (‰ versus PDB) − 10 × concentration of trimethoxycocaine]. Truxilline and trimethoxycocaine occur as two trace alkaloids in coca leaves. In addition to the obvious benefits for forensics, this illustration demonstrates the potential value of multi-isotope biomarker approaches for the geosciences to distinguish different geographical, climatological, and ecological regimes. Furthermore, it illustrates the importance of innovative data manipulation in biomarker research, especially when multiple isotope dimensions are employed. After *Ehleringer et al.* [2000].

Multi-element, Compound-specific Isotopic Analyses

Vanillin

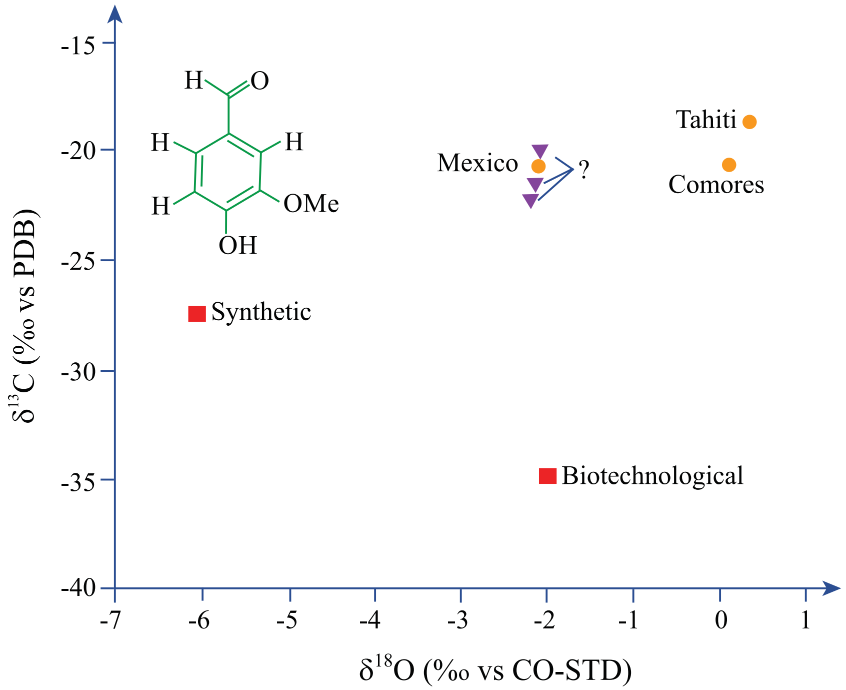

Dual isotopic ($\delta^{13}C$ and $\delta^{18}O$, in ‰ versus PDB and of standard CO, respectively) for the flavor compound vanillin. The three vanillin extracts from the naturally grown vanilla beans have similar $\delta^{13}C$ values, even though they come from geographically widely spaced sites: Mexico and the islands of the Comores and Tahiti. The Mexican sample, however, does differ markedly in $\delta^{18}O$, no doubt owing to major differences in $\delta^{18}O$ in the ambient water supply. Not surprisingly, major differences in both $\delta^{13}C$ and $\delta^{18}O$ are apparent in the synthetic and biotechnological products [*Hener et al., 1998*]. On the basis of their dual isotopic values, the three samples of unknown origin can be assigned to Mexico.

Figure by MIT OpenCourseWare.

Compound Specific Isotope Analysis

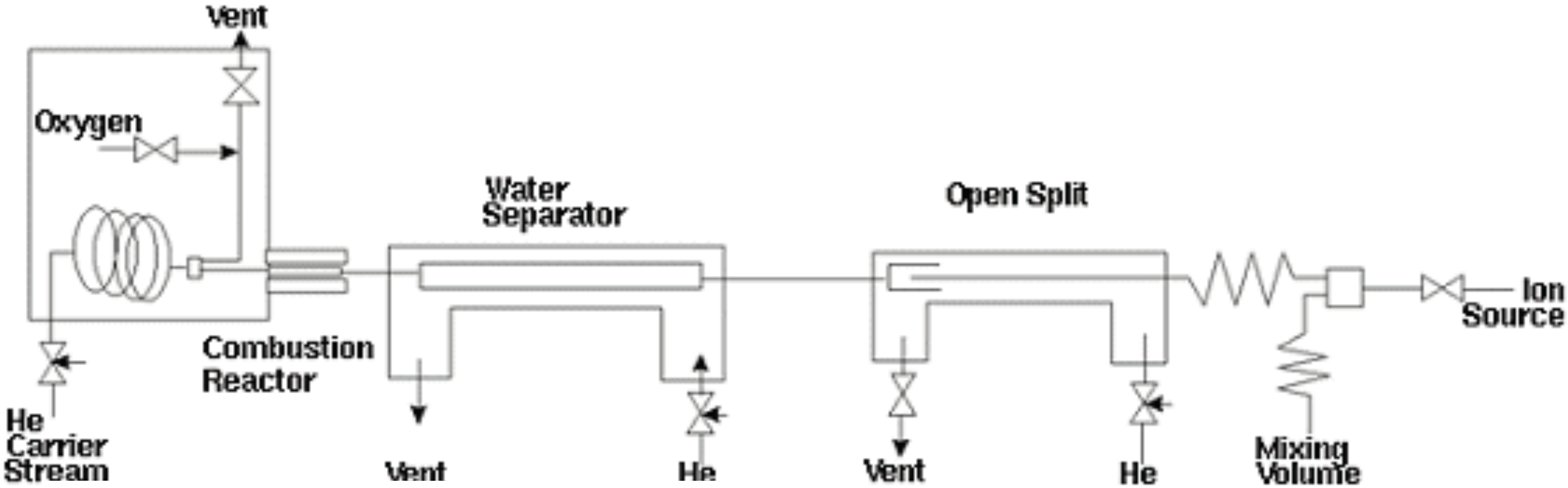

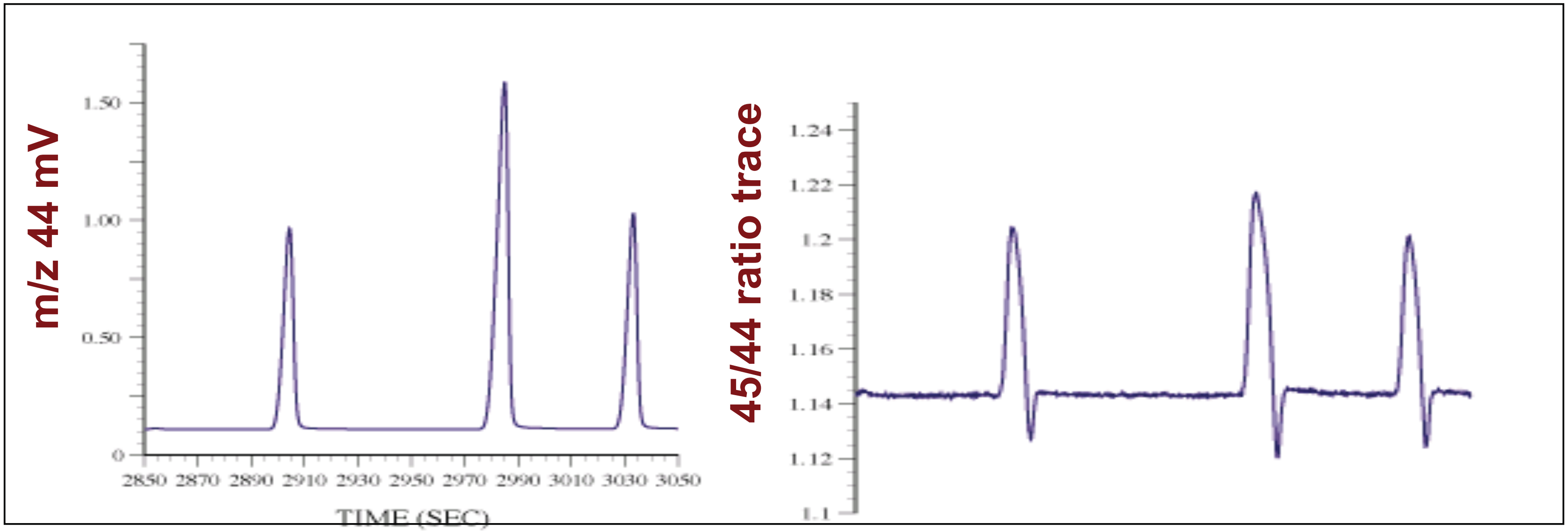

Courtesy of John Hayes. Used with permission.

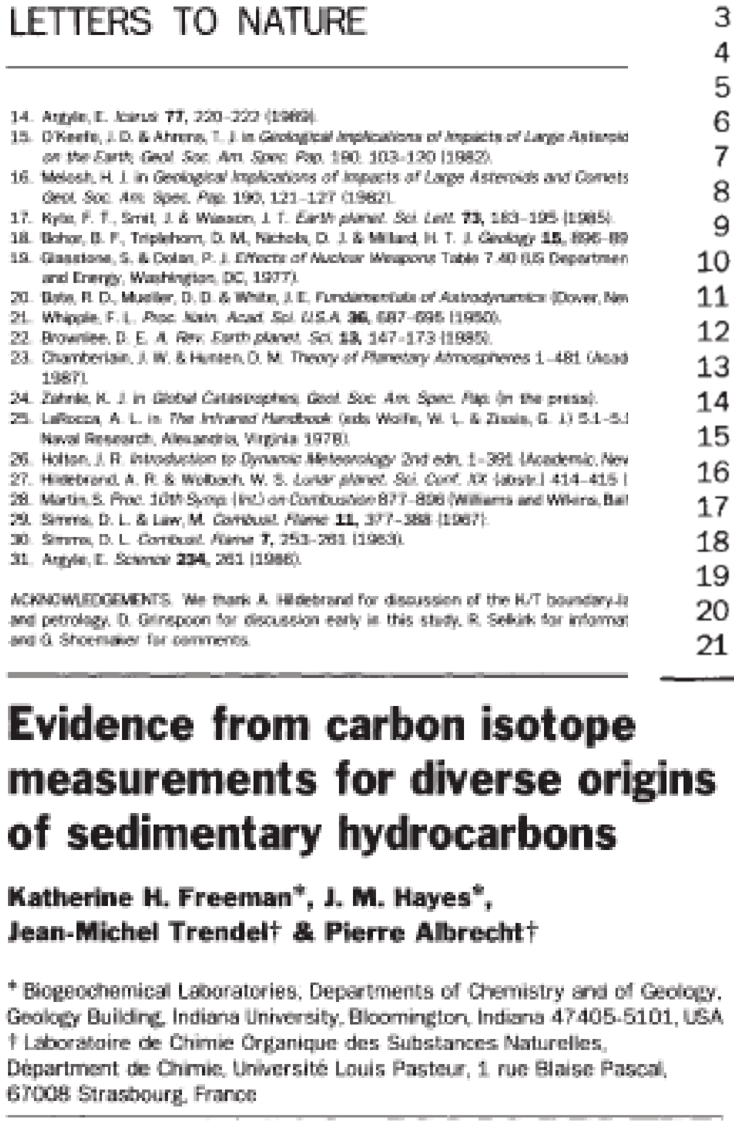

LETTERS TO NATURE

14. Argyle, E. *Icarus* **77**, 220–222 (1989).
15. O'Keefe, J. D. & Ahrens, T. J. in *Geological Implications of Impacts of Large Asteroid*
on the Earth, *Geol. Soc. Am. Spec. Pap.* 190, 103–120 (1982).
16. Melosh, H. J. in *Geological Implications of Impacts of Large Asteroids and Comets*
Geol. Soc. Am. Spec. Pap. 190, 121–127 (1982).
17. Kyte, F. T., Smit, J. & Wasson, J. T. *Earth planet. Sci. Lett.* **73**, 183–195 (1985).
18. Bohor, B. F., Triplehorn, D. M., Nichols, D. J. & Millard, H. T. *J. Geology* **15**, 896–89
19. Glasstone, S. & Dolan, P. J. *Effects of Nuclear Weapons* Table 7.40 (US Departmen
and Energy, Washington, DC, 1977).
20. Bate, R. D., Mueller, D. D. & White, J. E. *Fundamentals of Astrodynamics* (Dover, New
21. Whipple, F. L. *Proc. Natn. Acad. Sci. U.S.A.* **36**, 687–695 (1950).
22. Brownlee, D. E. *A. Rev. Earth planet. Sci.* **13**, 147–173 (1985).
23. Chamberlain, J. W. & Hunten, D. M. *Theory of Planetary Atmospheres* 1–481 (Acad
1987).
24. Zahnle, K. J. in *Global Catastrophes*, *Geol. Soc. Am. Spec. Pap.* (in the press).
25. LaRocca, A. L. in *The Infrared Handbook* (eds Wolfe, W. L. & Zissis, G. J.) 5.1–5.
Naval Research, Alexandria, Virginia 1978).
26. Holton, J. R. *Introduction to Dynamic Meteorology* 2nd edn, 1–391 (Academic, New
27. Hildebrand, A. R. & Wolbach, W. S. *Lunar planet. Sci. Conf. XX* (abstr.) 414–415 (
28. Martin, S. *Proc. 10th Symp. (Int.) on Combustion* 877–896 (Williams and Wilkins, Bal
29. Simms, D. L. & Law, M. *Combust. Flame* **11**, 377–388 (1967).
30. Simms, D. L. *Combust. Flame* **7**, 253–261 (1963).
31. Argyle, E. *Science* **234**, 261 (1986).

ACKNOWLEDGEMENTS. We thank A. Hildebrand for discussion of the K/T boundary la
and petrology, D. Grinspoon for discussion early in this study, R. Selkirk for informat
and G. Shoemaker for comments.

Evidence from carbon isotope measurements for diverse origins of sedimentary hydrocarbons

Katherine H. Freeman*, J. M. Hayes*,
Jean-Michel Trendel† & Pierre Albrecht†

* Biogeochemical Laboratories, Departments of Chemistry and of Geology,
Geology Building, Indiana University, Bloomington, Indiana 47405-5101, USA
† Laboratoire de Chimie Organique des Substances Naturelles,
Département de Chimie, Université Louis Pasteur, 1 rue Blaise Pascal,
67008 Strasbourg, France

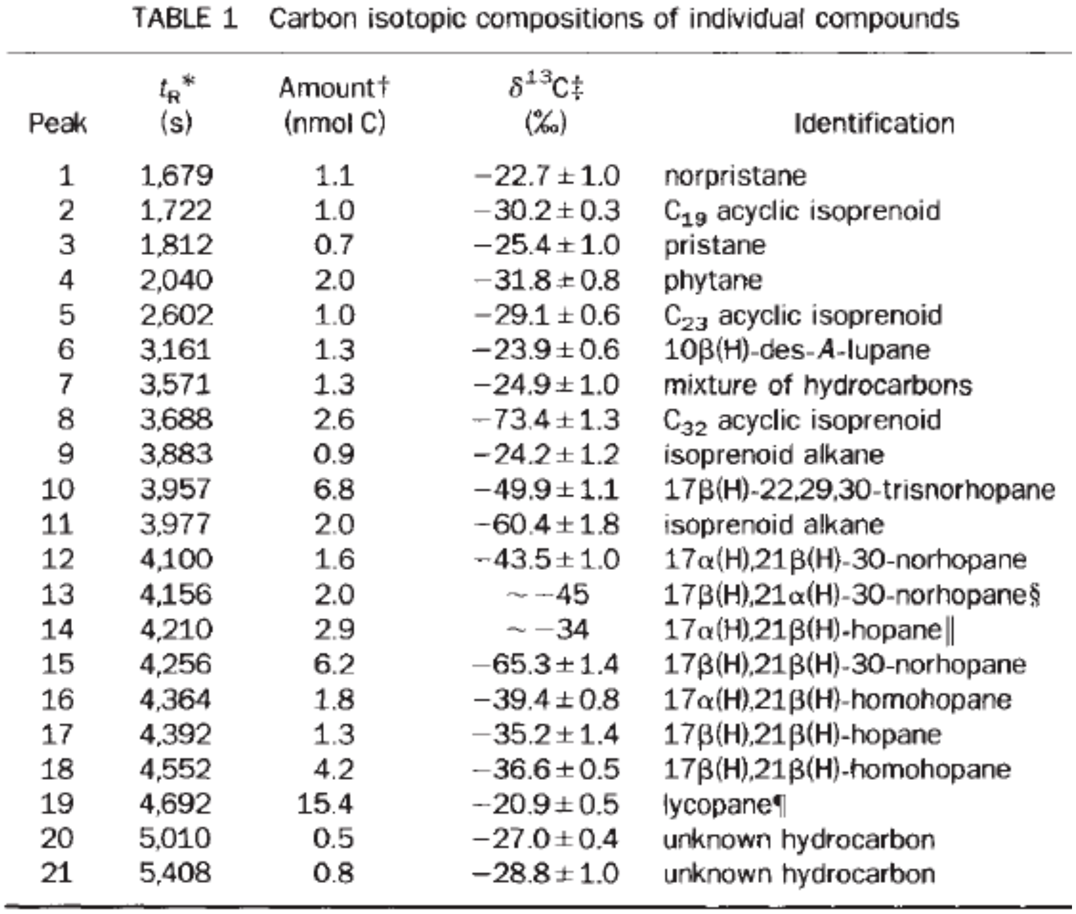

TABLE 1 Carbon isotopic compositions of individual compounds

Peak	t_R* (s)	Amount† (nmol C)	$\delta^{13}C$‡ (‰)	Identification
1	1,679	1.1	−22.7 ± 1.0	norpristane
2	1,722	1.0	−30.2 ± 0.3	C_{19} acyclic isoprenoid
3	1,812	0.7	−25.4 ± 1.0	pristane
4	2,040	2.0	−31.8 ± 0.8	phytane
5	2,602	1.0	−29.1 ± 0.6	C_{23} acyclic isoprenoid
6	3,161	1.3	−23.9 ± 0.6	10β(H)-des-*A*-lupane
7	3,571	1.3	−24.9 ± 1.0	mixture of hydrocarbons
8	3,688	2.6	−73.4 ± 1.3	C_{32} acyclic isoprenoid
9	3,883	0.9	−24.2 ± 1.2	isoprenoid alkane
10	3,957	6.8	−49.9 ± 1.1	17β(H)-22,29,30-trisnorhopane
11	3,977	2.0	−60.4 ± 1.8	isoprenoid alkane
12	4,100	1.6	−43.5 ± 1.0	17α(H),21β(H)-30-norhopane
13	4,156	2.0	~ −45	17β(H),21α(H)-30-norhopane§
14	4,210	2.9	~ −34	17α(H),21β(H)-hopane‖
15	4,256	6.2	−65.3 ± 1.4	17β(H),21β(H)-30-norhopane
16	4,364	1.8	−39.4 ± 0.8	17α(H),21β(H)-homohopane
17	4,392	1.3	−35.2 ± 1.4	17β(H),21β(H)-hopane
18	4,552	4.2	−36.6 ± 0.5	17β(H),21β(H)-homohopane
19	4,692	15.4	−20.9 ± 0.5	lycopane¶
20	5,010	0.5	−27.0 ± 0.4	unknown hydrocarbon
21	5,408	0.8	−28.8 ± 1.0	unknown hydrocarbon

Reprinted by permission from Macmillan Publishers Ltd. Katherine H. Freeman, J. M. Hayes, et al. Evidence from Carbon Isotope Measurements for Diverse Origins of Sedimentary Hydrocarbons. *Nature* 343 (1990): 254-6.

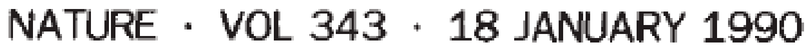

NATURE · VOL 343 · 18 JANUARY 1990

C-isotopic Composition of Organic Compounds

Three major controls

- Source of carbon and its C-isotopic composition
- Fractionation during assimilation (eg heterotrophy, photosynthesis, methanotrophy)
- Fractionation during biosynthesis (lipids)

C-isotopic Composition of Organic Compounds

Source of carbon and its C-isotopic composition

- Inorganic carbon
  - (-7‰ atm. CO_2) assimilated by photosynthesis

    ε → 5-35 per mil depending on pathway extent of consumption

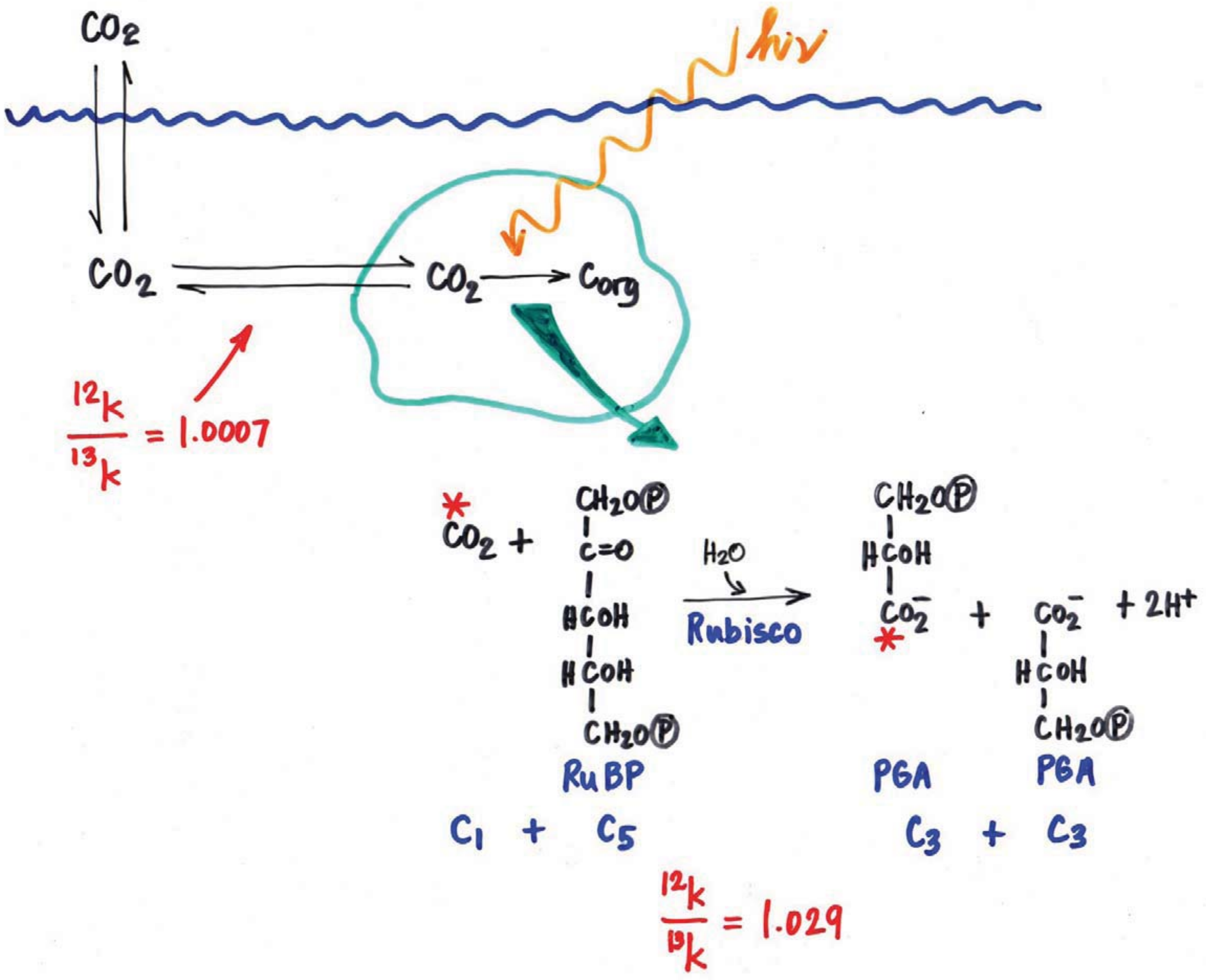
CO_2
$h\nu$
CO_2
$CO_2 \rightarrow C_{org}$
$\frac{^{12}k}{^{13}k} = 1.0007$
$\overset{*}{C}O_2$ +
CH_2OⓅ
C=O
HCOH
HCOH
CH_2OⓅ
H_2O
Rubisco
CH_2OⓅ
HCOH
CO_2^- *
+
CO_2^-
HCOH
CH_2OⓅ
$+ 2H^+$
RuBP
PGA
PGA
$C_1 + C_5$
$C_3 + C_3$
$\frac{^{12}k}{^{13}k} = 1.029$

C-isotopic Composition of Organic Compounds

- Fractionation during photosynthesis

Pathway, enzyme	**React & substr**	**Product**	ε ‰	**Organisms**
C3			10-22	
Rubisco1	CO_2 +RUBP	3-PGA x 2	30	plants & algae
Rubisco2	CO_2 +RUBP	3-PGA x 2	22	cyanobacteria
PEP carboxylase	HCO_3^- +PEP	oxaloacetate	2	plants & algae
PEP carboxykinase	CO_2 +PEP	oxaloacetate		plants & algae
C4 and CAM			2-15	
PEP carboxylase	HCO_3^- +PEP CO_2 +RUBP	oxaloacetate	2	plants & algae (C4)
Rubisco1		3-PGA x 2	30	
Acetyl-CoA			15-36	bacteria
CO dehydrog	CO_2 + 2H+ CoASH	AcSCoA	52	
Pyruvate synthase	CO2 + Ac-CoA	pyruvate		
PEP carboxylase	HCO_3^- +PEP	oxaloacetate	2	
PEP carboxykinase	CO_2 +PEP	Oxaloacetate		
Reductive or reverse TCA	CO2 + succinyl-CoA (+ others)	α-ketoglutarate	4-13	Bacteria esp green sulfur
3-hydroxypropionate	HCO_3^- + acetylCoA	Malonyl-CoA		Green non-S

Courtesy of John Hayes. Used with permission.

C-isotopic Composition of Organic Compounds

Source of carbon and its C-isotopic composition

- Inorganic carbon
  - (-7‰ atm. CO_2) assimilated by photosynthesis

    ε → 5-35 per mil depending on pathway extent of consumption
- Organic carbon
  - (-25‰ on average) assimilated during heterotrophy

    ε → -1 (you are what you eat plus 1 per mil!!)
- Methane carbon
  - (-30 to -100‰) assimilated during methanotrophy

    ε → 0-30 per mil depending on pathway and extent of consumption http://www.astrobio.net/news/modules.php?op=modload&name=News&file=article&sid=34

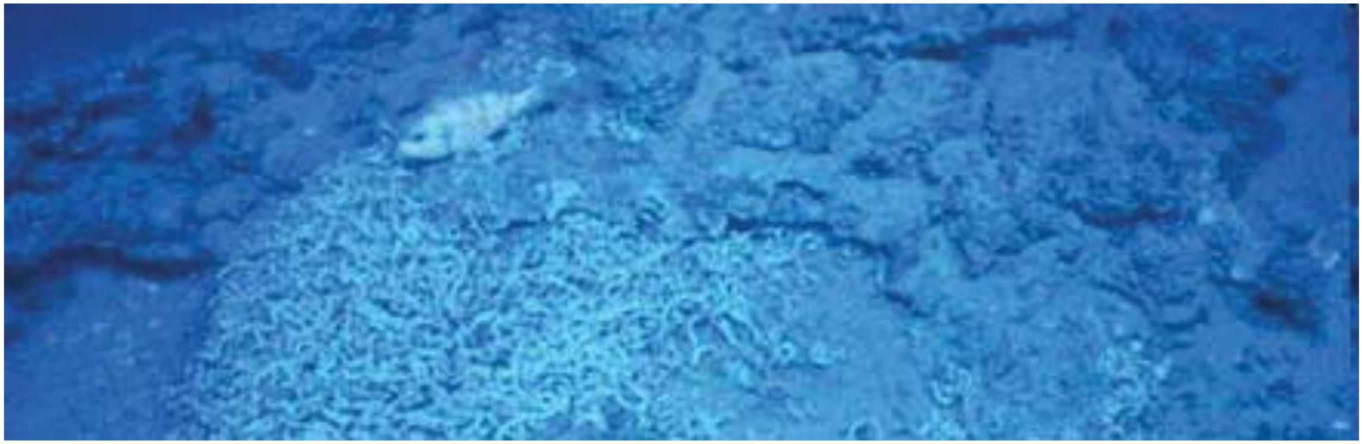

Café Methane

At the very edge of the brine pool, the mussels are especially abundant and happy. This area is often filled with newly settled baby mussels perched on the shells of larger mussels just above the brine.
Credit: Penn State University, Dept. of Biology

Gas hydrates (yellow) are ice with gas trapped inside; exposed beds are accessible to submersibles on the deep sea floor of the Gulf of Mexico. Ice worms, a new species only seen in hydrate, were discovered in 1997 by C. Fisher, Penn State University.

http://www.bio.psu.edu/People/Faculty/Fisher/cold_seeps/

Methane-rich water is pumped into the mussel and across its gills. The symbiotic bacteria in the gills use methane as both a carbon and energy source. The mussels, in turn, live off the symbiotic bacteria.

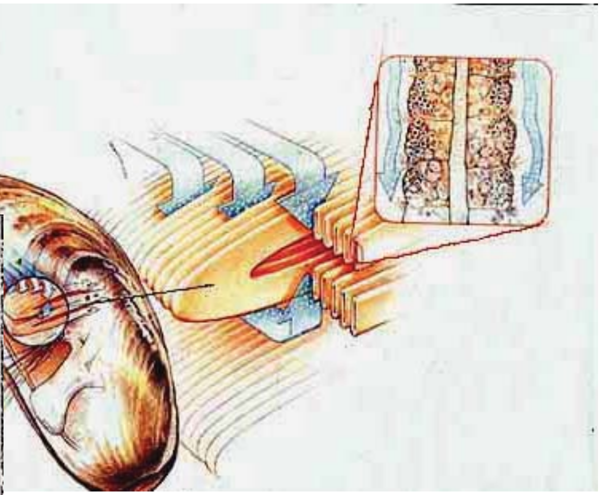

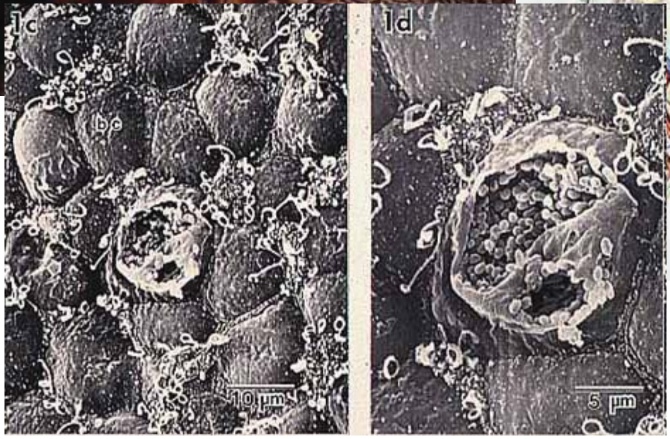

Using the scanning electron microscope, we can see over a dozen mussel gill cells in the panel on the left. On the right is a closer look at the cell with its outer membrane partially removed. Look into the cell to see hundreds of symbiotic bacteria.

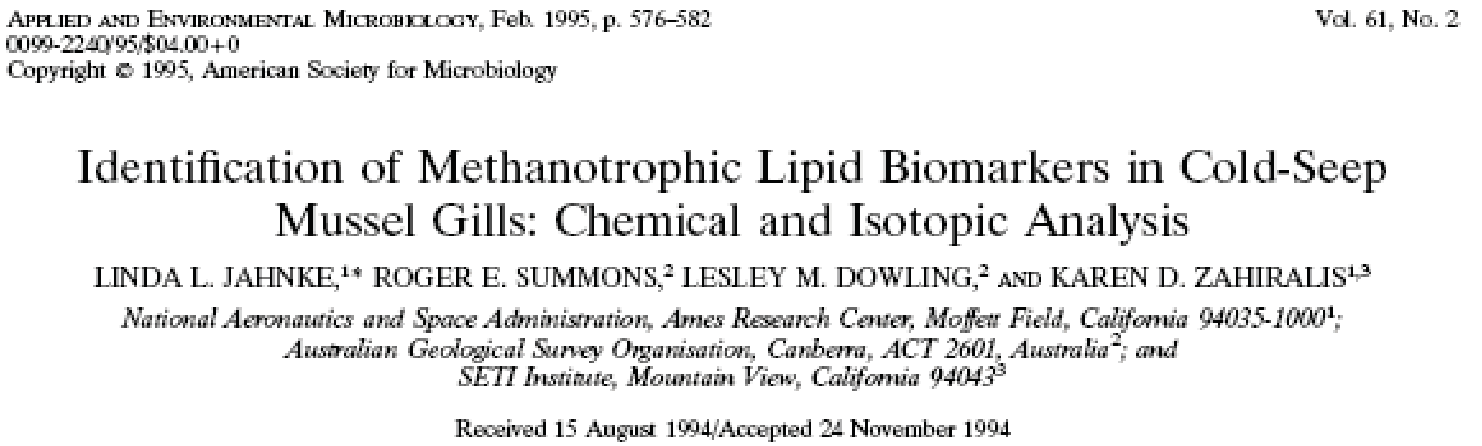

APPLIED AND ENVIRONMENTAL MICROBIOLOGY, Feb. 1995, p. 576–582 Vol. 61, No. 2
0099-2240/95/$04.00+0

Identification of Methanotrophic Lipid Biomarkers in Cold-Seep Mussel Gills: Chemical and Isotopic Analysis

LINDA L. JAHNKE,[1*] ROGER E. SUMMONS,[2] LESLEY M. DOWLING,[2] AND KAREN D. ZAHIRALIS[1,3]
National Aeronautics and Space Administration, Ames Research Center, Moffett Field, California 94035-1000[1]; Australian Geological Survey Organisation, Canberra, ACT 2601, Australia[2]; and SETI Institute, Mountain View, California 94043[3]

Received 15 August 1994/Accepted 24 November 1994

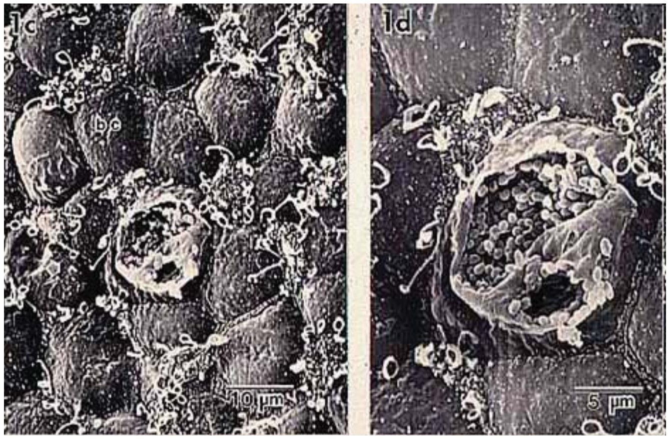

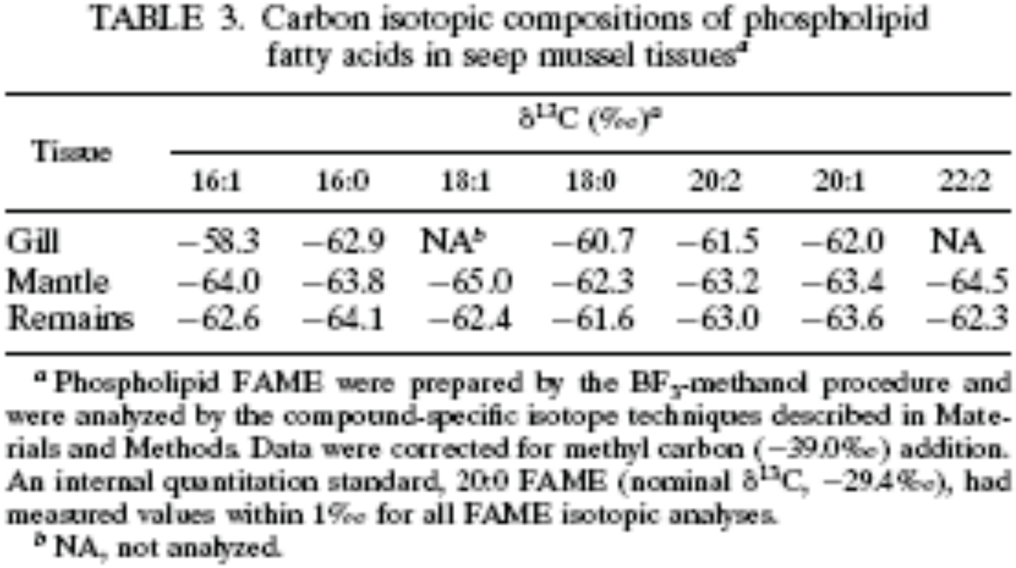

TABLE 3. Carbon isotopic compositions of phospholipid fatty acids in seep mussel tissues[a]

Tissue	$\delta^{13}C$ (‰)[a]						
	16:1	16:0	18:1	18:0	20:2	20:1	22:2
Gill	−58.3	−62.9	NA[b]	−60.7	−61.5	−62.0	NA
Mantle	−64.0	−63.8	−65.0	−62.3	−63.2	−63.4	−64.5
Remains	−62.6	−64.1	−62.4	−61.6	−63.0	−63.6	−62.3

[a] Phospholipid FAME were prepared by the BF_3-methanol procedure and were analyzed by the compound-specific isotope techniques described in Materials and Methods. Data were corrected for methyl carbon (−39.0‰) addition. An internal quantitation standard, 20:0 FAME (nominal $\delta^{13}C$, −29.4‰), had measured values within 1‰ for all FAME isotopic analyses.

[b] NA, not analyzed.

Using the scanning electron microscope, we can see over a dozen mussel gill cells in the panel on the left. On the right is a closer look at the cell with its outer membrane partially removed. Look into the cell to see hundreds of symbiotic bacteria.

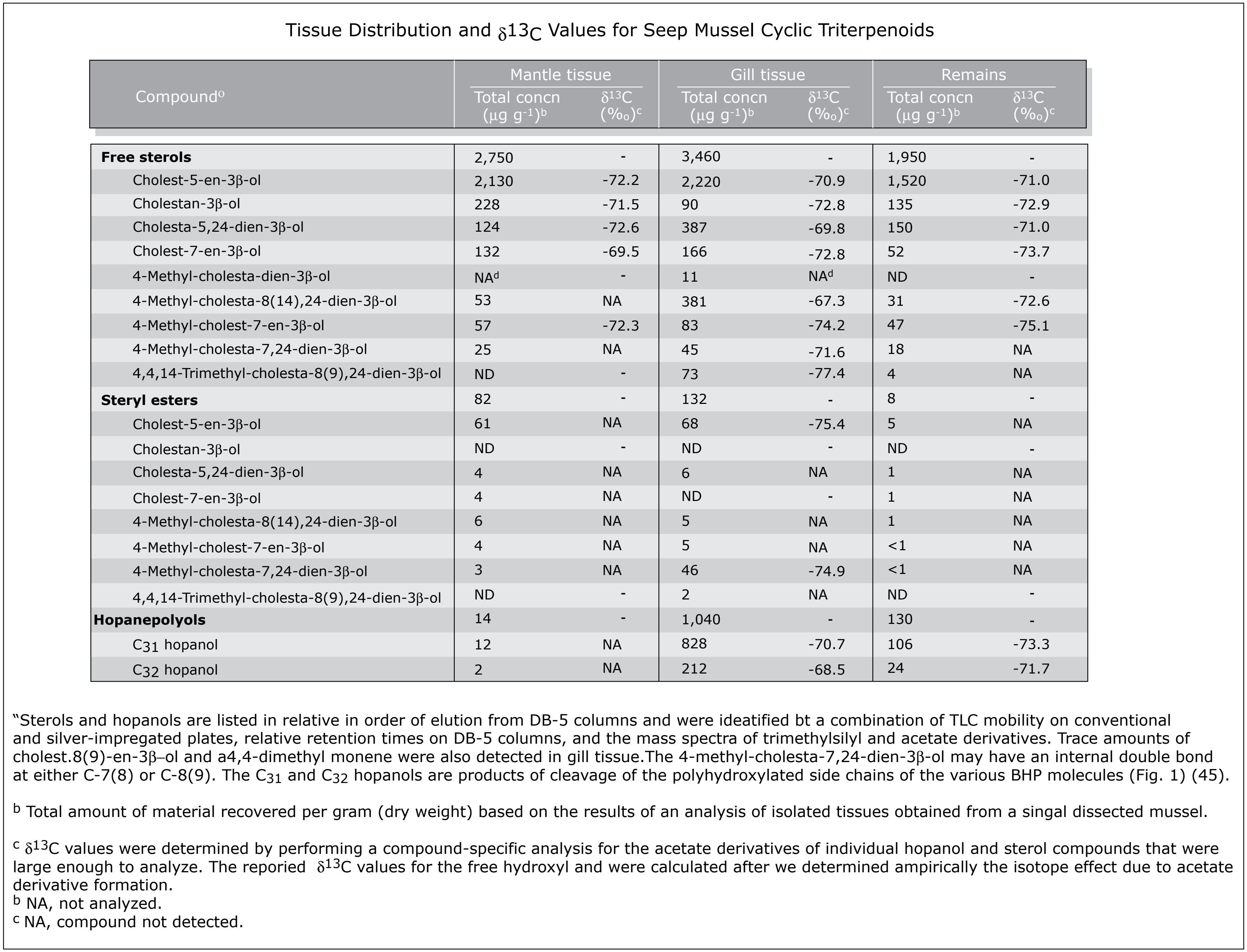

Tissue Distribution and δ13C Values for Seep Mussel Cyclic Triterpenoids

Compound[o]	Mantle tissue		Gill tissue		Remains	
	Total concn $(\mu g\ g^{-1})$[b]	δ^{13}C (‰)[c]	Total concn $(\mu g\ g^{-1})$[b]	δ^{13}C (‰)[c]	Total concn $(\mu g\ g^{-1})$[b]	δ^{13}C (‰)[c]
Free sterols	2,750	-	3,460	-	1,950	-
Cholest-5-en-3β-ol	2,130	-72.2	2,220	-70.9	1,520	-71.0
Cholestan-3β-ol	228	-71.5	90	-72.8	135	-72.9
Cholesta-5,24-dien-3β-ol	124	-72.6	387	-69.8	150	-71.0
Cholest-7-en-3β-ol	132	-69.5	166	-72.8	52	-73.7
4-Methyl-cholesta-dien-3β-ol	NA[d]	-	11	NA[d]	ND	-
4-Methyl-cholesta-8(14),24-dien-3β-ol	53	NA	381	-67.3	31	-72.6
4-Methyl-cholest-7-en-3β-ol	57	-72.3	83	-74.2	47	-75.1
4-Methyl-cholesta-7,24-dien-3β-ol	25	NA	45	-71.6	18	NA
4,4,14-Trimethyl-cholesta-8(9),24-dien-3β-ol	ND	-	73	-77.4	4	NA
Steryl esters	82	-	132	-	8	-
Cholest-5-en-3β-ol	61	NA	68	-75.4	5	NA
Cholestan-3β-ol	ND	-	ND	-	ND	-
Cholesta-5,24-dien-3β-ol	4	NA	6	NA	1	NA
Cholest-7-en-3β-ol	4	NA	ND	-	1	NA
4-Methyl-cholesta-8(14),24-dien-3β-ol	6	NA	5	NA	1	NA
4-Methyl-cholest-7-en-3β-ol	4	NA	5	NA	<1	NA
4-Methyl-cholesta-7,24-dien-3β-ol	3	NA	46	-74.9	<1	NA
4,4,14-Trimethyl-cholesta-8(9),24-dien-3β-ol	ND	-	2	NA	ND	-
Hopanepolyols	14	-	1,040	-	130	-
C_{31} hopanol	12	NA	828	-70.7	106	-73.3
C_{32} hopanol	2	NA	212	-68.5	24	-71.7

“Sterols and hopanols are listed in relative in order of elution from DB-5 columns and were ideatified bt a combination of TLC mobility on conventional and silver-impregated plates, relative retention times on DB-5 columns, and the mass spectra of trimethylsilyl and acetate derivatives. Trace amounts of cholest.8(9)-en-3β–ol and a4,4-dimethyl monene were also detected in gill tissue.The 4-methyl-cholesta-7,24-dien-3β-ol may have an internal double bond at either C-7(8) or C-8(9). The C_{31} and C_{32} hopanols are products of cleavage of the polyhydroxylated side chains of the various BHP molecules (Fig. 1) (45).

[b] Total amount of material recovered per gram (dry weight) based on the results of an analysis of isolated tissues obtained from a singal dissected mussel.

[c] δ^{13}C values were determined by performing a compound-specific analysis for the acetate derivatives of individual hopanol and sterol compounds that were large enough to analyze. The reporied δ^{13}C values for the free hydroxyl and were calculated after we determined ampirically the isotope effect due to acetate derivative formation.
[b] NA, not analyzed.
[c] NA, compound not detected.

Image by MIT OpenCourseWare.

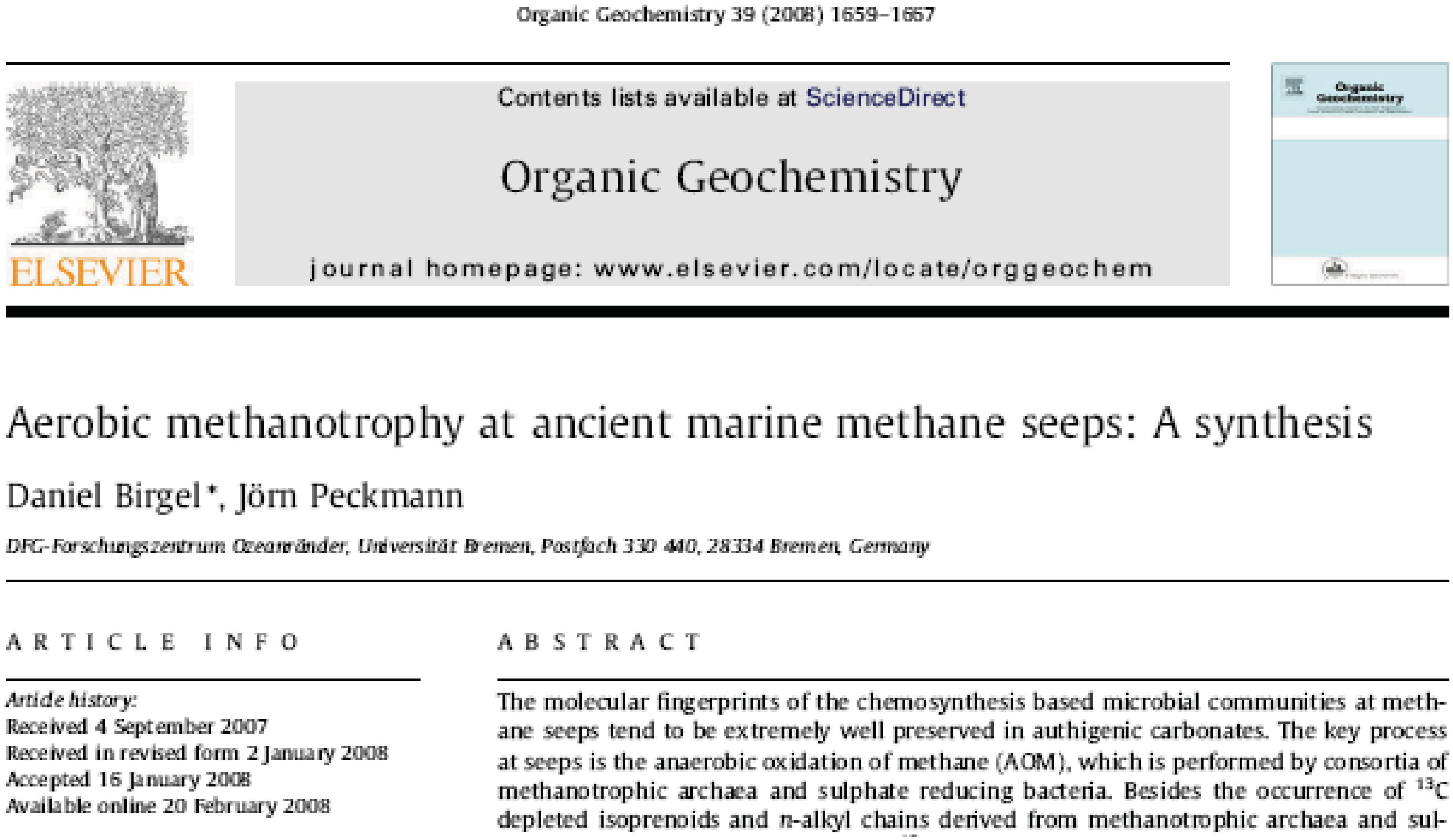

Organic Geochemistry 39 (2008) 1659–1667

Contents lists available at ScienceDirect

Organic Geochemistry

journal homepage: www.elsevier.com/locate/orggeochem

Aerobic methanotrophy at ancient marine methane seeps: A synthesis

Daniel Birgel*, Jörn Peckmann

DFG-Forschungszentrum Ozeanränder, Universität Bremen, Postfach 330 440, 28334 Bremen, Germany

ARTICLE INFO

Article history:
Received 4 September 2007
Received in revised form 2 January 2008
Accepted 16 January 2008
Available online 20 February 2008

ABSTRACT

The molecular fingerprints of the chemosynthesis based microbial communities at methane seeps tend to be extremely well preserved in authigenic carbonates. The key process at seeps is the anaerobic oxidation of methane (AOM), which is performed by consortia of methanotrophic archaea and sulphate reducing bacteria. Besides the occurrence of ^{13}C depleted isoprenoids and *n*-alkyl chains derived from methanotrophic archaea and sul-

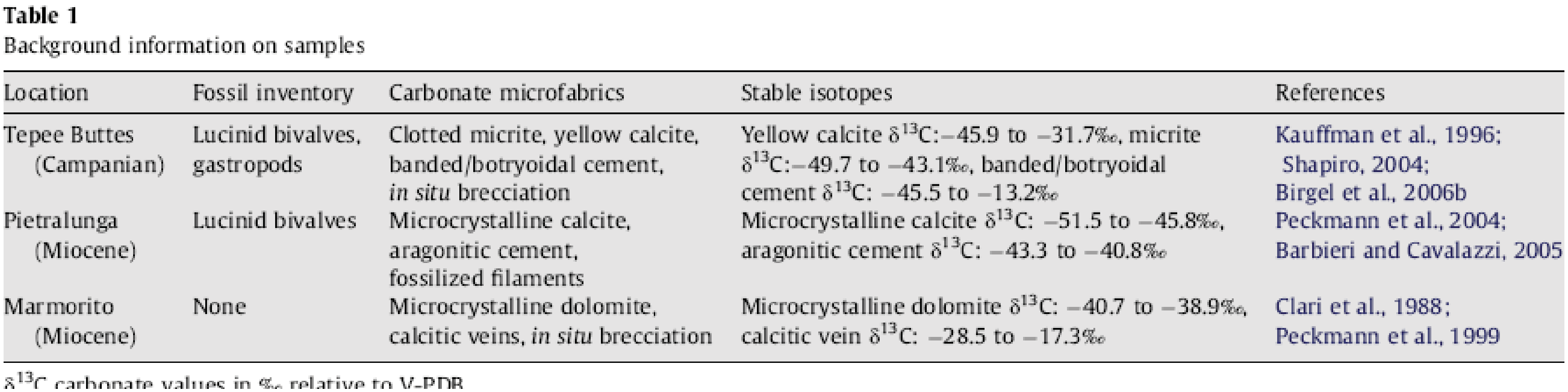

Table 1
Background information on samples

Location	Fossil inventory	Carbonate microfabrics	Stable isotopes	References
Tepee Buttes (Campanian)	Lucinid bivalves, gastropods	Clotted micrite, yellow calcite, banded/botryoidal cement, *in situ* brecciation	Yellow calcite δ^{13}C:−45.9 to −31.7‰, micrite δ^{13}C:−49.7 to −43.1‰, banded/botryoidal cement δ^{13}C: −45.5 to −13.2‰	Kauffman et al., 1996; Shapiro, 2004; Birgel et al., 2006b
Pietralunga (Miocene)	Lucinid bivalves	Microcrystalline calcite, aragonitic cement, fossilized filaments	Microcrystalline calcite δ^{13}C: −51.5 to −45.8‰, aragonitic cement δ^{13}C: −43.3 to −40.8‰	Peckmann et al., 2004; Barbieri and Cavalazzi, 2005
Marmorito (Miocene)	None	Microcrystalline dolomite, calcitic veins, *in situ* brecciation	Microcrystalline dolomite δ^{13}C: −40.7 to −38.9‰, calcitic vein δ^{13}C: −28.5 to −17.3‰	Clari et al., 1988; Peckmann et al., 1999

δ^{13}C carbonate values in ‰ relative to V-PDB

hop-17-(21)-ene XII; δ^{13}C: -32‰)

Lanostane (XVIII; δ^{13}C: -70‰)

Norlanostane (XVII; δ^{13}C: -80‰),

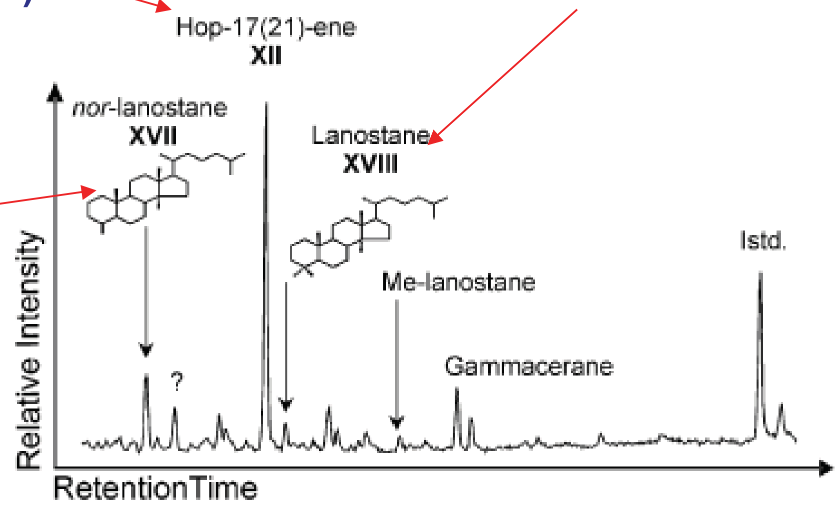

Fig. 1. Partial gas chromatogram (total Ion Current: TIC) of hydrocarbon fraction from Pietralunga. Istd.: internal standard. Roman numbers: see Appendix.

Courtesy Elsevier, Inc., http://www.sciencedirect.com. Used with permission.

C-isotopic Composition of Organic Compounds

- Fractionation during biosynthesis (lipids)

C-isotopic compositions of amino acids from Anabeanea grown on different N-sources (Macko et al., 1987)

Isotopic enrichment of carboxyl carbon relative to remainder of molecule. Amino acids from eight microbial cultures.

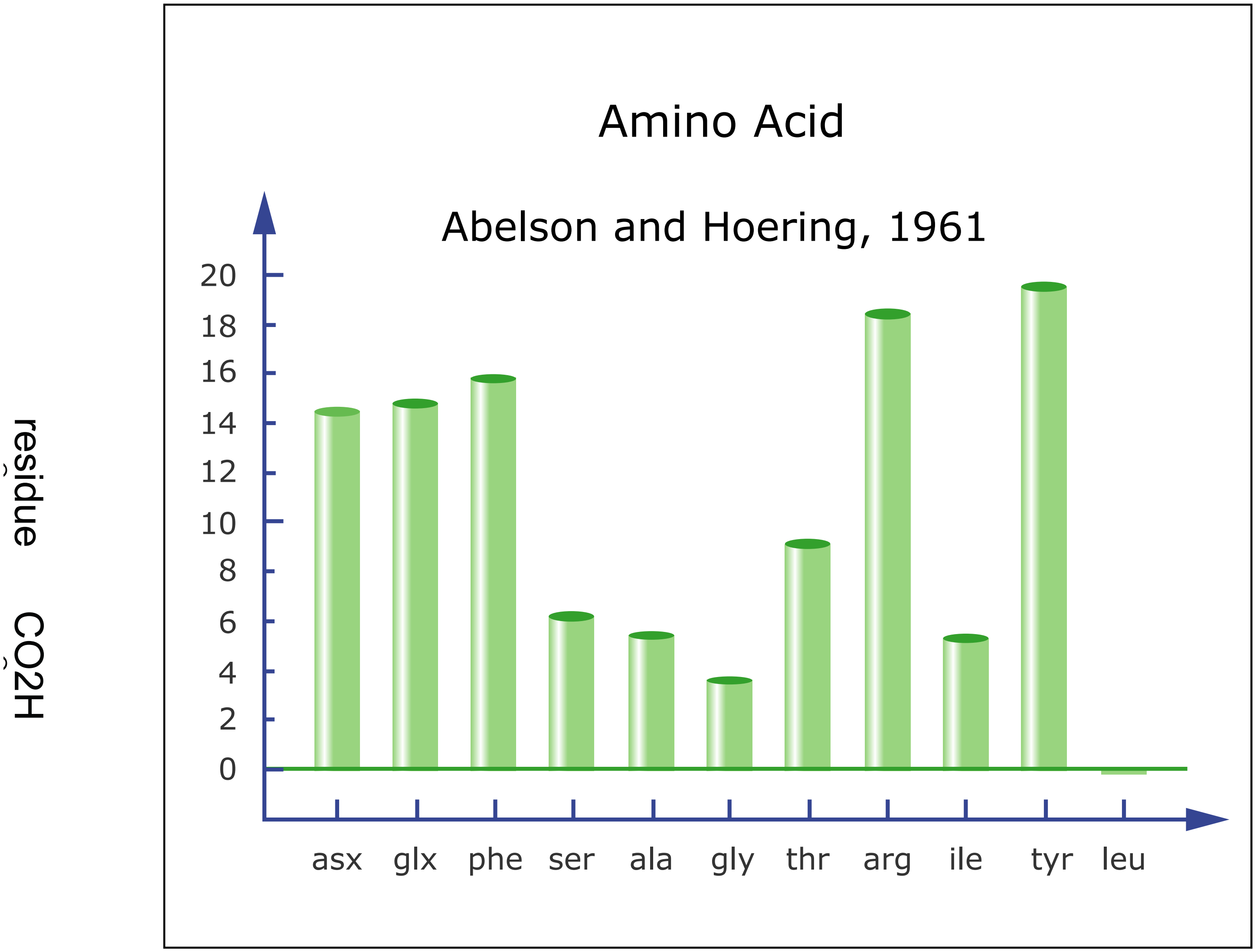

Image by MIT OpenCourseWare.

Intramolecular C-isotopic Differences

(DeNiro and Epstein, 1977; Monson and Hayes, 1980, 1982; reviewed Hayes, 2001)

Reactions occur between molecules but isotope selectivity is expressed as chemical bonds that are made or broken at particular carbon positions.

Isotope effects pertain to those specific positions and control fractionations only at that reaction site, not throughout the whole molecule.

To calculate changes in the isotopic compositions of whole molecules we must first calculate the change at the site and then allow for the rest of the molecule because the isotopic shift is diluted by mixing with carbon that is just along for the ride………………..Hayes, 2002

Isotopic Fractionations in Biosynthetic Reactions

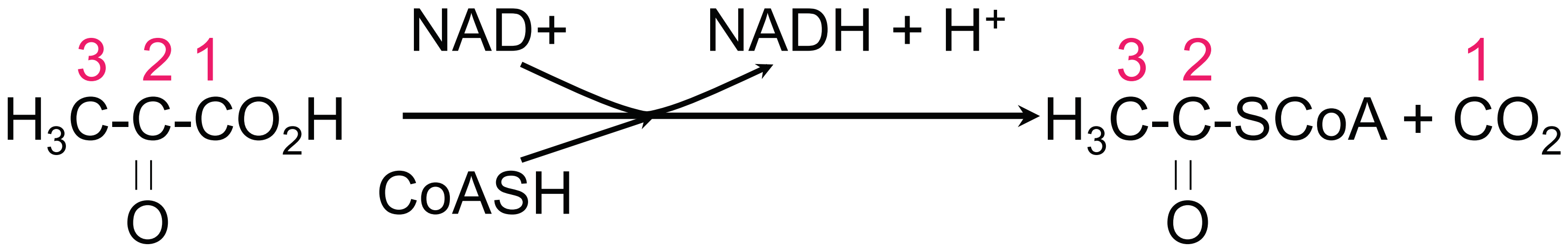

$$\overset{3}{H_3C}\text{-}\underset{\overset{||}{O}}{\overset{2}{C}}\text{-}\overset{1}{CO_2H} \xrightarrow[\text{CoASH}]{\text{NAD+} \qquad \text{NADH + H}^+} \overset{3}{H_3C}\text{-}\underset{\overset{||}{O}}{\overset{2}{C}}\text{-}SCoA + \overset{1}{CO_2}$$

Pyruvate Dehydrogenase

$$({}^{12}K/{}^{13}K)_{C\text{-}2} = 1.0232$$

The species containing carbon-12 at position 2 reacts **1.0232 times** more rapidly that the species containing carbon-13 at that position

It is termed “a 23‰ isotope effect”

Flows of C at the pyruvate branch point in the metabolism of E. coli grown aerobically on glucose (Roberts 1955). 74% of the pyruvate is decarboxylated to yield Ac-CoA. The observed depletion at odd-numbered positions of FAcids is shown at the right indicating that the isotope effect at C-2 in the pyruvate dehydrogenase reaction is 23‰

D/H by GC–pyrolysis–IRMS

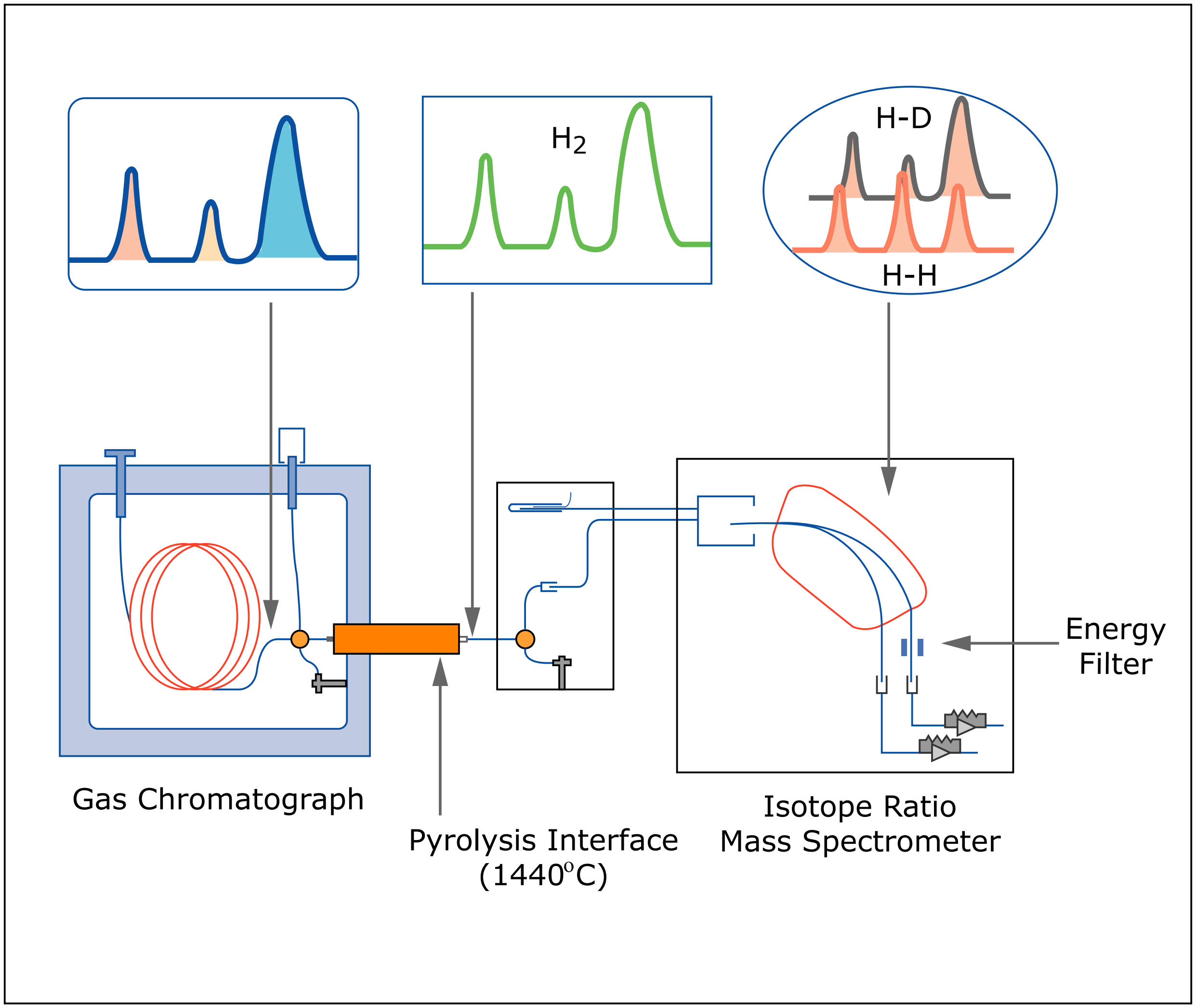

Image by MIT OpenCourseWare.

Hilkert, 1998; Burgoyne, 1998; Sessions, 1999

12.007 Geology
Spring 2013